SAPIENZA
UNIVERSITÀ DI ROMA

PhD Course in Molecular Medicine

XXXVI cycle

Coordinator Prof. Giuseppe Giannini

The MYC 5' upstream region facilitates autophagic adaptations in response to PI3K inhibition

Candidate

Devon Michael Ivy

Matricola 1976265

Tutor

Prof. Gianluca Canettieri, M.D., Ph.D.

A.A. 2022-2023

ACKNOWLEDGEMENTS

The success of this thesis could not have been possible without the motivation and support from a great many people. I am extremely grateful for Professor Canettieri inviting me to perform my doctoral studies in his laboratory and supervising my training during this period. I would also like to thank Rosa Bordone, who I have had a great pleasure of working with on this project and was instrumental in the achievement of this thesis as well as navigating the challenges of being international.

I would also like to thank Professor Bournias-Vardiabasis for her guidance during my Master of Science, and it was the opportunities you provided me that started my career in research. A special thank you to Tate and Sarah, for their belief in me and my abilities, and being there for me when times were tough. I must also thank my parents. Your support never wavered from the peaks to the troughs my life, and nothing I have accomplished could have been done without you.

Table of Contents

ABSTRACT

The internal ribosome entry site (IRES) is considered one of the mechanisms in which colorectal cancer cells can utilize to survive the stresses of the tumor microenvironment and to escape cell death. The proto-oncogene MYC is upregulated in 70% of human neoplasia and is considered a key driver of colorectal cancer (CRC). An IRES sequence was discovered in its 5' UTR, presenting the possibility of tumoral cells utilizing this mechanism to sustain cell growth under stressful conditions. However, controversy exists surrounding the technical approaches used to validate this sequence. We investigated the involvement of the MYC IRES in a diverse range of cellular stresses using a CRIPS-Cas9 approach to excise the sequence from CRC cell lines. Our results demonstrate that the MYC IRES does not facilitate cap-independent translation. Rather, it appears to function as transcriptional enhancer responsive to PI3K signaling mediated through the MAP-kinase pathway. CRC cells adapt to PI3K inhibition by increasing the autophagic flux, however, those cells lacking the IRES fail to do so, and demonstrate antiproliferative sensitivity. This sensitivity is also found in Burkitt Lymphoma (BL) cells that exhibit a MYC translocation dissociating the IRES from the coding sequence. In conclusion, we find that the MYC IRES functions not to facilitate internal ribosome entry, but to enhance MYC

transcription in response to PI3K inhibition in order to promote cancer cell survival though increased autophagic flux.

INTRODUCTION

Colorectal cancer

Colorectal cancer (CRC) is a leading health care burden worldwide. In the United States of America alone, CRC has the second most expensive treatment cost of all cancer at $24.3 billion, representing 12.6% of the cost of all cancer treatments in 2020[1]. According to the World Health Organization, it compromises roughly 10% of the 19.3 million global cancer cases in 2020[2]. In the context of patient mortality, it ranks as the second most deadly, claiming every year over a million lives[2].

CRC was originally modeled by Fearon and Vogelstein as a multi-step accumulation of genetic activations in oncogenes and mutational inactivation of onco-suppressor genes, and that mutational activation of at least four to five genes were required for the formation of a malignant tumor[3]. In recent years, through the efforts accumulating far reaching genetic data such as The Cancer Genome Atlas, much information regarding the dysregulation of major signaling pathways and accumulation of mutations has been obtained[4,5]. The shared reporting of gene-expression data among researchers has allowed for the discovery of extensive molecular characterization of the disease. CRC is

highly heterogeneous with regards to genetic signature, and has been classified into different consensus molecular subtypes (CMS)[6] based on their defining genetic signatures: CMS1, microsatellite instability immune; CMS2, canonical with WNT and MYC signaling activations; CMS3, epithelial and metabolic dysregulation; and CMS4, mesenchymal and high transforming growth factor-β activation; samples with mixed signatures are suggested to represent a transitional phenotype of heterogeneity within the tumor itself[6].

These classifications have assisted in the treatment and prognosis of CRC. High microsatellite instability/mismatch repair deficient tumors (MSI-H), for example, fall into CMS1. These tumors have been found to be highly susceptible to immunotherapy, and the Food and Drug Administration (FDA) of the United States of America has approved antibody-based PD-L1 (programmed cell death-ligand 1) therapies, such as pembrolizumab[7] and nivolumab[8], and other immune checkpoint inhibitors blocking therapy that functions by preventing cells from escaping immune surveillance in patients exhibiting high MSI-H[9]. This therapy has had a significant degree of success thus far and is highly promising. However, the MSI-H phenotype only represents a small proportion of individuals with CRC at 15%[10], indicating a dire need to address the other subtypes. Chromosomal instability (CIN) is a mechanism of genetic dysregulation, categorizing as CMS2, and represents the largest proportion of patients with CRC from 60 to 85%[11], and with a

worse prognosis[12] compared to MSI. Genomic instability caused by CIN results in aneuploidy and loss of heterozygosity, as well as a high prevalence of mutations in genes that coordinate signals for cell proliferation, survival, and cell cycle regulation[13].

Genes implicit in the CIN phenotype of colorectal cancer

Despite the high heterogeneity of CIN, in most cases, the proto-oncogene MYC is overexpressed[14]. The reason for this can be due to many of the aberrantly regulated signaling pathways in CIN converging on MYC. For example, mutations of *APC* occur early in the tumor-progression process[3], resulting in stability of β-catenin and its translocation into the nucleus, which then activates the Wnt signaling pathway[15]. Commonly followed by *APC* mutations is *KRAS*[13]; these two mutations together can promote tumor progression *in vivo*[16], a pathway utilizing MEK and converging onto MYC expression and stabalization[17]. Other mutations occur in inhibiting the tumor suppressor genes *TP53 or PTEN* or activating the oncogenes *KRAS* and *PIK3CA*[13].

The gravity of MYC in the development of intestinal tumors is well demonstrated in $APC^{MIN/+}$ mice[18]. These mice, which overexpress MYC, reliably develop 30-50 intestinal tumors by the end of their life cycle. *In vivo*

knock out of MYC in $APC^{MIN/+}$ mice have abrogated tumor development entirely[19].

The proto-oncogene MYC

The proto-oncogene MYC is a master transcriptional regulator of numerous cellular processes, in particular of cellular metabolism, as well as cell proliferation, cell growth[20], and apoptosis. A basic helix-loop-helix leucine zipper, MYC functions by first forming a heterodimer with MAX[21] and subsequently binding to regions of the DNA known as E-Box sites; its canonical target sequencing being 5'-CACGTG-3'[22,23]. MYC can control both transcriptional activation and repression depending on its target gene, and both processes are heavily dependent on epigenetic modifications of the immediate chromatin[24–26] to allow for MYC binding and modulatory activity. The frequency of E-Box sequences is high throughout the human genome, allowing for MYC to regulate roughly 15% of all genes[27]. MYC was first discovered to contain oncogenic potential in the context of Burkitt Lymphoma, where its translocation under the control of the IG enhancer elements[28,29] resulted in constitutive activation and oncogenesis.

The MYC promoter

The *MYC* locus contains a highly complex and transcribed promoter that facilitates its regulation by a number of converging signaling pathways, including JAK/STAT and MAPK signaling in addition to the aforementioned WNT. *MYC* contains four different promoters termed P0, P1, P2, and P3[30–32]. P0 is the furthest upstream in the MYC locus. P1 and P2 are the proximal promoter sequences located 161 bases apart from each other, and roughly

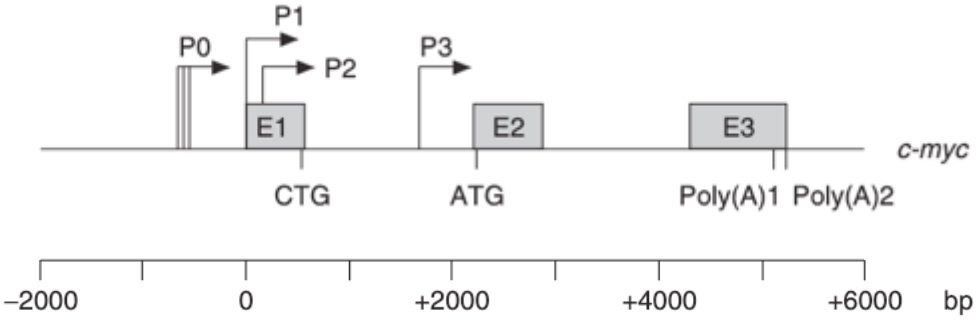

The MYC locus and organization of the promoter regions. Wierstra, Inken (2008). [Advances in Cancer Research] Volume 99 || The c-myc Promoter: Still MysterY and Challenge, 113–333. doi:10.1016/S0065-230X(07)99004-1

500 bases upstream the MYC coding sequence (CDS), and compromise of 10-25/75-90% of MYC mRNA content, respectively. Promoter site P3 resides within intron 1 of MYC. P2 activity dominates and is attributed to its optimal TATA-box[33–35]. The P1/P2 TATA-box promoter regions also are the subject of the converging signal regulation. While P1/P2 code for ~95% of MYC mRNA content together, P0/P3 code for 0-5% under typical conditions, particularly due to their lack of TATA boxes and lack of other promoter elements[36].

Challenges drugging MYC

Under homeostatic conditions, expression of MYC is tightly regulated[37–39]. However, MYC shows extensive dysregulation and/or upregulated in ~70% of human neoplasia[39,40] and is a major cause of human mortality[41]. Aberrantly activated MYC confers a selective growth advantage to cancer cells by rewiring both transcriptional programs and signaling modules. For its involvement in multiple cancers and mortality, MYC is a desirable target for cancer therapy. Much effort, both clinical and preclinical, have been dedicated towards strategies at limit its dysregulated expression. However, to this day there exists no approved pharmacological inhibitor of MYC. There exist two main reasons for this: one due to the structure of MYC. MYC is a helix-loop-helix protein, and therefore possess a flat structure and consequently lacks druggable pockets and clefts. As MYC mechanically dimerizes with either MAX or MYC for its biological function, attention has been drawn towards preventing this purpose. Second, the side effects of MYC inhibition are expected to be systemic and severe. MYC is expressed throughout the human body[42,43]; any non-specific inhibition towards cancer cells can result in dangerous and intolerable systemic side-effects.

Due to these difficulties, other strategies are also being investigated towards alleviating the aberrant intracellular levels of MYC. Downstream targets of MYC, such as polyamine biosynthesis[44], represent some of these efforts[45]. Other approaches target the different stages of MYC biosynthesis, such as its transcription, or translation[46,47]. Drugs targeting MYC protein synthesis have been tested both preclinically and in humans, providing promising results[48].

Canonical translation

The initiation of canonical eukaryotic translation is a complex coordination of at least a dozen known translation factors[49] that begins when 7-methyl-guanosine (m^7GpppN, cap) is recognized and bound by the subunit eIF4E of the eIF4F translation initiation complex[50]. eIF4E then guides the pre-initiation complex to the mRNA, which then scans and begins translation at typically the first AUG codon it encounters.

The binding of eIF4E is regulated tightly by the eIF4E binding protein, 4E-BP. 4E-BP has high affinity for eIF4E and upon binding, it prevents eIF4E from binding to the 5' cap of mRNA. When 4E-BP is phosphorylated, it is unable to bind eIF4E, which permits eIF4E to bind mRNA and begin the

initiation of translation. 4E-BP phosphorylation occurs by a number of kinases, and the mechanistic target of rapamycin (mTOR) in particular[51].

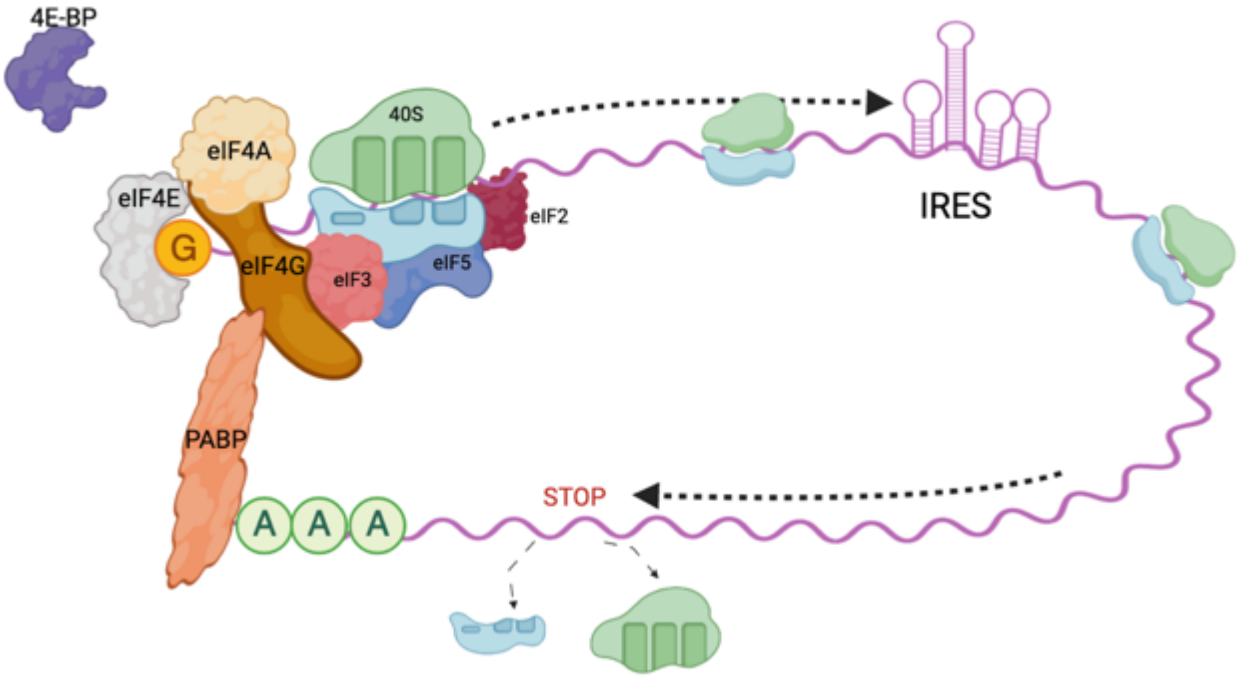

Canonical initiation of translation. Image created in BioRender.

Non-canonical translation

The ability for cells to initiate translation canonically is compromised in various conditions. Not all of these conditions result from stress, mitosis being one example. Other conditions are much more stressful or critical for survival at an organismal level, such as infection, and others, such as oxidative stress and nutritional depletion. However, in these conditions, specific transcripts

can still be translated and produce normal, functionally active proteins[52]. In some of these transcripts there exists a highly structured region known as an internal ribosome entry site (IRES), which can facilitate ribosomal entry and translation independently of some or all of the translation initiation factors. The internal ribosome entry site is suggested to be a mechanism that can overcome the difficult conditions in which a tumor can face[53–57], and are most commonly observed in both viral and eukaryotic genomes.

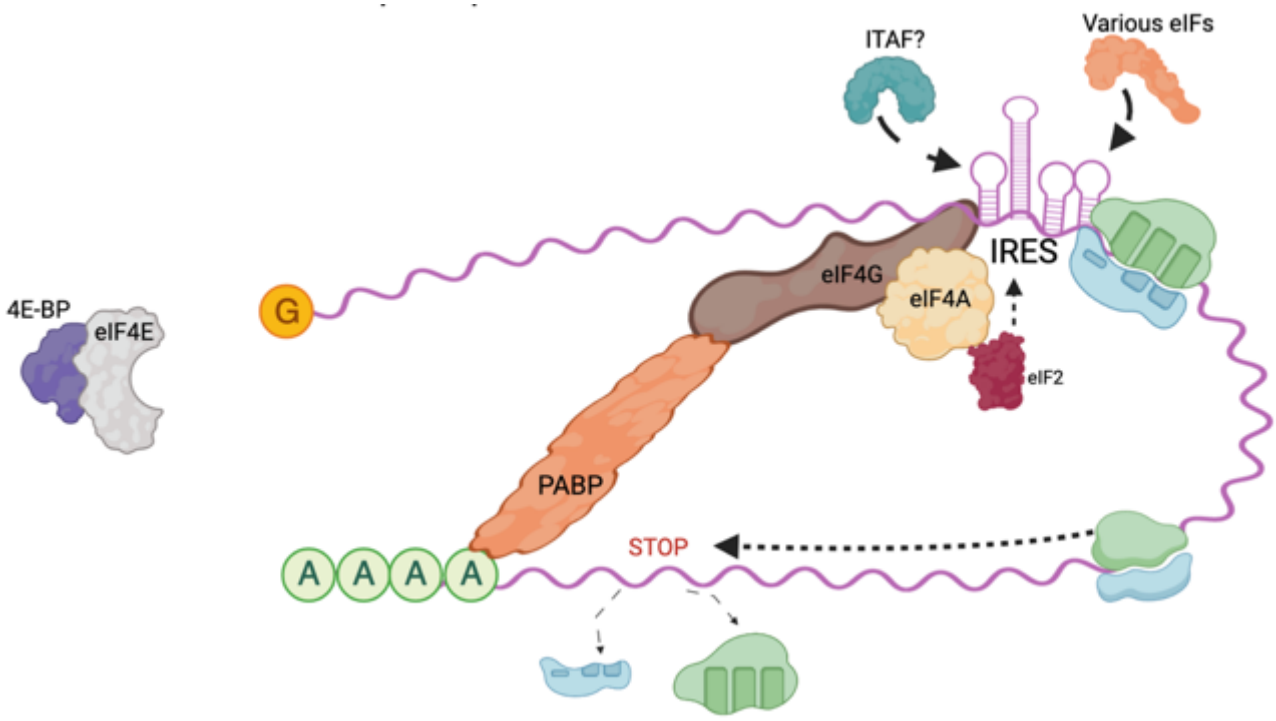

Non-canonical initiation of translation. The ribosomes initiate translation without the binding of eIF4E. Image created in BioRender.

Internal-ribosome entry site (IRES)

IRES elements were first discovered in the context of picornaviruses and encephalomyocarditis viruses[58–60], which could begin translation of their

own genome when their host cell inhibited translation due to the presence of its own infection. Some viral RNA genomes, such as the poliovirus, do not contain a 5' cap, which naturally demands an alternative method to initiate translation of its genome[61]. The IRES is a region in the mRNA, typically on its 5' end, that is able to bind directly to the ribosome and initiate translation. Even when the RNA circularized *in vitro*, viral IRES elements are also able to bind ribosomes, and can be translated[62].

The viral IRES is diverse across different viral genomes, yet exhibits some similarities[63,64], and can be broadly defined as able to initiate translation without needing eIF4E to bind the mRNA. To varying degrees, viral IRES elements rely on host factors to assist in the initiation of translation. However, this degree varies greatly, and in the most extreme of cases, there is no requirement for any host factors at all[65]. In addition to host translation factor requirements, viral IRES elements can be categorized based on their secondary structure, the ability to directly bind the 40S ribosomal subunit, and ITAF (IRES *trans*-acting factor) recruitment, which are proteins required to start translation but are *not* part of the initiation machinery[66]. These details allow for the classification of viral IRES elements into four different groups[67].

The mechanism in which viral IRES elements function is well understood. Group 1 viral IRES elements initiate translation from a non-AUG start codon, and this occurs from the ribosome's A-site rather than the P-

site[68]. Group 1 viral IRES elements require no host initiation factors (a feature hypothesized due to the group's IRES secondary structure[61]), and are generally close to the downstream open reading frame of the viral genome[69]. Group 2 viral IRES elements are much more complex with regards to secondary structure, and contain overall more nucleotides than group 1[70]. They also do not require ITAFs, however, they have critical requirement of eIF2 and eIF3 to initiate translation. Groups 3 and 4, increasingly complex in their secondary structures, both require ITAFs to bind the 60S ribosome (group 4 has an AUG-scanning mechanism) and have an extended requirement in general for initiation actors. Overall, viral IRES elements are able to robustly facilitate translation of proteins including cases where the viral mRNA is not capped[71], proving a highly reliable mechanism to force translation of its mRNA under conditions in which a cell's defense would otherwise try to prevent this.

The cellular IRES

The existence and function of cellular IRES elements is controversial and heavily debated. Cellular IRES elements lack the sequence and structural homology that identifies their viral counterparts, making their identification challenging[67]. Similarly, even for the cellular IRES elements that

have had sizable evidence in favor of their existence, they do not translate proteins nearly as robustly as their viral counterparts[72]. Originally, cellular IRES elements were discovered with a technique known as the dicistronic reporter assay. In this assay, exogenous DNA with two luciferase genes (for example Renilla and Firefly luciferase), separated by the DNA region of interest, is transfected into a cell. This DNA region of interest would be a putative IRES. In this reporter construct, translation coming from the 5' luciferase gene would occur via a cap-dependent initiation mechanism. Hypothetically, as the ribosome dissociates form the monocistronic mRNA due to encountering a stop codon at the end of the first cistron, and therefore, any observable signal originating from the 3' luciferase gene downstream would have to be due to internal ribosome entry at the putative IRES sequence. However, this technique has been shown to have pitfalls. The popular pRF plasmid used to conduct these assays was found to have a cryptic promoter[73], producing an alternative 3' cistron transcript not in a cap-*independent* manner, and rendering the results of such dicistronic experiments unreliable. Many experiments utilizing these constructs did not include sufficient analyses to conclude the vectors used did not produce unintended mRNA[72]. In many cases, follow-up experiments frequently find splicing and other cryptic promoter activity[72,74–77].

Adding to the unreliability of the dicistronic reporter assay for validating IRES elements, it has been found that the ability to demonstrate internal ribosome initiation depends highly on the choice of surrounding genes, even with viral IRES elements[78]. Another problem with reporting IRES activity is the masking of true efficiency using relative results[72]. Many IRES elements have been found to produce activity as low as 3-6% of control "empty vector" levels, or even viral IRES sequences used as control[79–81]. The sequences found as IRES elements are by-and-large highly inefficient at translating proteins, and any luciferase signal reporting a 3-fold represents still a very minor fraction of total protein content. A problem persists in addressing any physiological role for this minor amount of product, or whether it simply remains experimental background. Considering the viral IRES functions sufficiently for their purpose[72], this evidence suggests the cellular IRES element might not functionally provide for cellular demands under times of stress.

The MYC IRES

MYC was shown to have an IRES in the late 1990s and early 2000s[82–84], and suggested to play a role in chemoresistance[85]. This region, found within exon 1, has been defined to reside from the nucleotide positions -363

to -94 upstream from the first start codon in exon 1 of MYC. Coincidentally, this overlaps with the exact nucleotides starting the P2 promoter element of MYC[83]. However, the evidence for the MYC IRES originates from using pRF plasmids and dicistronic RNA constructs, calling into question the validity of these claims. Adding to the controversy, when the MYC IRES was tested in response to various stresses in a different vector than the pRF plasmid – a βgal/CAT vector - there was a significant reduction in activity compared to controls, a result inconsistent with it functioning as an IRES[86]. Furthermore, another research group evidence presented suggested the region is *not* an IRES through the use of circularized mRNA. If the MYC IRES could facilitate cap-independent translation, it would be able to do so in a circularized mRNA, which naturally have no 5' or 3' ends–it failed to do so, whereas the HSP70 IRES succeeded[87].

Hypothesis

In this thesis, I address the involvement of the MYC IRES in response to various stresses, and whether it facilitates internal ribosome entry and translation of MYC protein independently of the cap-binding mechanism. In order to probe whether the MYC IRES could facilitate protein expression under various stresses, we utilized the CRISPR/Cas9 method to excise the

IRES from colorectal cancer cells. To functionally demonstrate IRES activity *in vitro*, we utilized monocistronic mRNA-based luciferase reporter constructs to avoid the pitfalls of DNA-based transfection of dicistronic reporters and to avoid cryptic splicing events that can occur to dicistronic mRNA reporter constructs. We found and delineated a role for the IRES sequence in a genomic context, functioning as a key regulatory element enhancing MYC transcription in response to PI3K inhibition. The enhancement of MYC transcription resulted in an increase of MYC protein content in a cap-dependent fashion that then led to an autophagic adaptation, a mechanism which CRC cells utilize to survive class I PI3K inhibition. We also found that cancer cells lacking the MYC IRES are unable to induce this autophagic adaptation - particularly relevant in Burkitt Lymphoma, where some patient-specific cases lose the transcriptional regulatory elements in the translocated MYC gene, including the IRES. These results overall suggest a role for the IRES in a genomic context as a functional responsive element to class I PI3K inhibition.

MATERIAL AND METHODS

Cell culture and drug treatments

HCT116 and SW620 colorectal cancer cells were cultured in Dulbecco's Modified Eagles Medium (DMEM; Sigma-Aldrich #D6546) with a supplementation of 10% fetal bovine serum, 1% penicillin-streptomycin (100 U/mL each), and 1% L-glutamine. Raji and DG75 cells were a gift from Professor Pankaj Trivedi at Sapienza University of Rome. Raji and DG75 cells were cultured in RPMI-1640 (Sigma #R0883) supplemented with 10% fetal bovine serum, 1% penicillin-streptomycin (100 U/mL each), and 1% L-glutamine. All cell lines were cultured in a cell incubator at 37°C and 5% CO_2. All cell lines used were confirmed mycoplasma-free via PCR using a Mycoplasma PCR detection Kit (Applied Biological Materials, Inc. #G238).

Drug treatments were performed using thapsigargin (Sigma Aldrich #T9033), doxorubicin (Sigma Aldrich #D1515), 5-fluorouracil (Sigma Aldrich #F6627), 2-deoxy-2-glucose (2DG; Sigma #D8375), H_2O_2 (Santa Cruz Biotechnology #7722-84-1), BEZ235 (Cayman Chemicals #10565), BKM120 (MedChemExpress #HY-70063), cycloheximide (Sigma Aldrich #C4859), actinomycin D (Sigma Aldrich #A4262), U0126 (Promega #V1121) at the indicated concentrations in the text. Cells were incubated with cycloheximide for 1 hour. Drugs were suspended in dimethyl sulfoxide (DMSO) unless otherwise stated. All cell treatments with the listed drugs were 24 hours long,

unless indicated otherwise in the text. Treatments for proliferation assays were for the entire length of the assay and refreshed every 48 hours.

Proliferation Assays

Cells were seeded in a Multi-Well 12 (Corning 3513) at a density of 20,000/cm^2. The next day, cells were treated with the drugs indicated in the text. Cells were counted daily via tryphan blue staining. Lymphoma cells for 7-day proliferation counts were seeded in a Multi-Well 12 at a density of 1,000/cm^2. The drugs and media were refreshed every 3 days.

Mice Experiments

All animals were housed following the Italian Ministry of Health Directive 2010/637EU guidelines. Female NU/NU CD1 mice (28-34 days old) (Charles River Laboratories #086NU/NUCD) were housed in standard conditions of 12h light/12h dark cycle, at a constant temperature of 19-22°C, 45% humidity, and with availability of food and water *ad libitium*. HCT116 SCR and ΔIRES cells were cultured $2.0x10^6$ cells were prepared in a 50 µL solution of 50% Matrigel (Corning #354248) and 50% PBS which was injected subcutaneously into each posterior flank of the nude mice. Animal health and xenografted cells were monitored daily. Once the tumors were palpable,

animals were administered BKM120 (30 mg/kg) or vehicle (90% corn oil/10% DMSO) via oral gavage daily for 15 days. Every 3 days, the dimensions of each tumor were recorded. Volume was calculated as $V = (L \times W^2)/2$ as previously described[88]. At 15 days, animals were sacrificed via cervical dislocation, and the tumor masses were excised, weighed, photographed, and collected for molecular analyses.

Immunohistochemistry

Freshly excised xenografted tumors were fixated in 4% paraformaldehyde for 24 hours at 4°C and transferred to 1X PBS the following day. Samples were embedded in paraffin wax after dehydration in increasing ethanol concentrations and washed with xylenes. 5 µm-think cross sections were prepared using a RM2245 microtome (Leica Biosystems). The deparaffinized and rehydrated sections had antigens retrieved using 1X Tris-EDTA, pH 9.0 solution, pH 9.0 (Himedia #ML087) for 30 minutes at 95°-98°C on a hot plate. Sections were stained using the Mouse-to-Mouse Kit by ScyTek Laboratories (#MTM001): First, samples were blocked with Super Block for five minutes and then with mouse-to-mouse block for 30 minutes. Sections were then incubated with primary antibodies as listed in Table 1 in a solution of 1X PBS with 1% bovine serum albumin. The next day, sections were quenched with 3% hydrogen peroxide in methanol for 20 minutes.

Afterwards, a biotinylated goat anti-polyvalent peroxidase was applied for 30 minutes at room temperature, followed by streptavidin-conjugated horseradish peroxidase. The chromogenic reaction was developed using 3,3'-diaminobenzidine tetrahydrochloride (DAB) solution. Nuclei were counterstained with Mayer's hematoxylin (Sigma-Aldrich #MHS16). Eosin (Histo-Line Laboratories #DV002153) was used following standard protocols. Representative images of each sample/stain were captured at 20x original magnification by a Zeiss Axiocam 208 color on a Zeiss Axiolab 5 light microscope.

Confocal Microscopy

Cells were seeded in an µ-Slide 8 Well ibiTreat cell culture dish (ibidi #80826) at 50,000/cm^2. LysoTracker red was used following manufacturer's instructions. 62x normal magnification confocal images were acquired using a LSM 980 with Airyscan 2 (Zeiss) laser-scanning confocal microscope.

Plasmids and antibodies

Lentiviral plasmids for RNA interference and CRISPR/Cas-9-mediated gene excisions were generated in pLKO.1 (AddGene #8453) and pLentiCRISPR-v2 (AddGene #52961), respectively. The shRNA and sgRNA sequences used are listed in Table 2. Complementary oligonucleotides were

phosphorylated using PNK (Takara Bio #2021B) and annealed by submerging in boiling water and then allowing the temperature to reach 25°C over 4 hours. Annealed oligonucleotides were ligated using Takara T4 DNA Ligase (Takara Bio #6021) in the corresponding digested vectors.

For *in vitro* transcription, the Firefly luciferase coding region was PCR amplified from pGL3 basic (Promega #E1751) and cloned in pSP64-polyA (Promega #P1241) using XbaI (ThermoFisher #ER0681) and BamHI (ThermoFisher #ER0051) restriction sites. MYC 5' UTR (IRES) was PCR amplified from HCT116 cDNA and cloned in pSP64-Poly A (Promega #P1241) using HindIII (ThermoFisher #ER0502) and XbaI restriction sites. To insert the hairpin sequence in the vector upstream the MYC 5' UTR, HindIII was used. Complementary oligonucleotides were phosphorylated, annealed, and ligated in the digested vectors with and without the MYC 5' UTR (IRES). All constructs were validated by sequencing.

For the HBM-IRES-Luciferase construct, the MYC IRES was PCR amplified from HCT116 cDNA and cloned into HBM-Luciferase (AddGene #35155) using NotI (ThermoFisher #ER0591) restriction sites.

All antibodies used for immunoblotting are listed in Table 1.

In Vitro transcription

pSP64-Poly A derived plasmids were *in vitro* transcribed using HiScribe SP6 RNA Synthesis Kit (NEB #E2070S). Plasmids were linearized by digestion with EcoRI and after purified via Phenol:Chloroform extraction. The synthesis reaction was prepared according to the manufacturer's protocol and cap ($m^7G(5')ppp(5')G$ RNA Cap Structure Analog (NEB #S1404S) or AP3G (ApppG, Jena Bioscience #72655) were added to a final concentration of 4 mM and incubated at 37°C in a PCR thermocycler for 30 minutes. Transcripts were treated with DNAse I, purified by LiCl precipitation, and quantified using a NanoPhotometer (Implen #NP80).

Luciferase assays

HCT116 cells were seeded at a density of $5.0*10^4$ cells/cm^2 in a Multi-Well 24 dish (Corning #) in triplicate. The following day, cells were treated with BKM120 [1 μM] or an equal volume of dimethyl sulfoxide (DMSO) for 24 hours. The next day, 400 ng per well of *in vitro* transcribed RNA were transfected using DreamFect transfection reagent (OZ Biosciences #DF41000) according to the manufacturer's protocol. After 6 hours, cells were collected and washed with 0.1 M PBS with Mg^{2+} and Ca^{2+}. Cell extracts were then prepared with passive lysis buffer (Biotium, #99912) according to the manufacturer's protocol; D-luciferin (Biotium #10101) was diluted in the

noncommercial stock luciferase assay buffer as previously described[89] with a final concentration of 40 mg/mL. Luminescence was read with a Glomax Explorer Multimode Microplate Reader (Promega #GM3500). Luciferase units were normalized to the efficiency of transfection as monitored by RT-qPCR.

CRISPR/Cas-9-mediated deletion of the MYC IRES

The MYC IRES was excised using small guide RNA (sgRNA) targeting the region -363 to -94 base-pairs upstream the non-canonical CTG start codon[82,83]. The sequences are described in Table 2. For transient expression of Cas9 and sgRNAs, HCT116 and SW620 cells were transfected with the constructs and selected with puromycin (Enzo Life Sciences #ALX-380-028) for 72 hours, then diluted into 96-well plates to allow monoclonal growth, collected, and screened via PCR using the screening primers described in Table 2. The clones identified as homozygous ΔIRES were then subjected to Sanger sequencing (Bio-Fab Research).

Polysomal fractionation

HCT116 and SW620 cells were processed and MYC mRNA distribution in the differing polysomal fractions were analyzed as described[45,90]. Briefly, cells were treated with 100 µg/ml cycloheximide (CHX) for 5 minutes, washed twice with 1X PBS, and subsequently lysed with 450 µl of TNM lysis buffer

(10 mM Tris-HCl pH 7.4 or 7.5, 10 mM NaCl, 10 mM $MgCl_2$, 1% Triton X-100) supplemented with 10 mM dithiothreitol, 100 µg/ml CHX, 1× PIC (#1187358001 complete, EDTA free, Roche, Mannheim Germany), and RiboLock RNase inhibitor (#EO0382 Thermo Fisher Scientific, Burlington, ON, Canada). Lysates were incubated on ice for 10 min and then centrifuged. Supernatants were collected, loaded onto a 15–50% sucrose gradient, and ultracentrifugation was performed at 37,000 RPM for 120 min with a SW41 rotor (Beckman Coulter, Brea, CA). Fractions collection was performed using Biorad-BioLogic LP/2110 (Hercules, California,USA), according to the manufacturer's protocol. Synthetic RNA was used as a normalization control for RT-qPCR. 1 ng was added to the pooled fractions immediately before RNA extraction. The oligos used for quantitative PCR are listed in Table 2. The synthetic RNA was transcribed *in vitro,* and the sequence is as follows: 5' GAAATTAATACGACTCACTATAGGATCGAGGTCTAGCTATAGGATTAGGA TCGTCGTAGTTAGAAAGTATGGAGAAAGGAAGCGCTTCTCTGAAGGCTG GGGCTTTATGATTGCTGCTAAGTTTGCTGAAAGGGATGGAAAGTGATGC TAGCTGAGTGAGTGATCGAGCTAGGTA 3'.

Western blot

Cells were lysed in the denaturing buffer SDS-urea (50 mM Tris HCl, pH 7.8, 2% sodium dodecyl sulfate (SDS), 10% glycerol, 10 mM $Na_4P_2O_7$,

100 mM NaF, 6 M urea, 10 mM Ethylenediaminetetraacetic acid (EDTA)). Protein extracts were then sonicated, quantified, and resolved via SDS-PAGE before transfer toa nitrocellulose membrane (Perkin Elmer, #NBA085C001EA). Membranes were blocked with 5% milk powder in 0.1 M tris buffered saline with 0.1% Tween-20 (TBS-T) and incubated in the same buffer with primary antibodies overnight. The following day, membranes were washed in TBS-T and subsequently incubated with secondary antibodies for 1 hour. Detection of the horseradish peroxidase signal was performed using WesternBright ECL (Advansta, #K-12045-D50).

RNA extraction, reverse transcription, and quantitative PCR (RT-qPCR)

Total mRNA was isolated from cells using Trizol reagent (ThermoFisher #15596026) according to the manufacturer's instructions. 1 µg of total RNA was reverse-transcribed with SensiFAST^{TM} cDNA Synthesis Kit (Meridian Bioscience #BIO-65053). Real-time PCR was performed using SensiFast Sybr Lo-Rox Mix (Meridian Bioscience #BIO-94020) and transcript levels were quantified with a ViiA 7 Real-Time PCR System 36 instrument (Applied Biosystems). The primers used are listed in Table 2.

Lentivirus-mediated shRNA knockdown and overexpression

The production of lentiviruses was performed as described[91]. Subconfluent HEK-293T cells were co-transfected, by calcium phosphate precipitation[92], with 20 µg of different pLKO.1 vectors together with 15 µg of pCMV-R 8.74 (AddGeme #22036), and 10 µg of pMD.G2 (AddGeme #12259) to produce lentiviruses. After 24 hours, the medium was changed. Supernatant containing recombinant lentiviruses was collected 72h after transfection.

To perform lentiviral transduction, cells were seeded at a density of 2.0 * 10^4 cells/cm^2 and transduced with lentiviruses the next day with polybrene (5 mg/mL, Sigma-Aldrich #H9268). Knockdown efficiency was monitored by RT-qPCR. Cells were infected for 72 hours and then were selected via puromycin for 72 hours.

Statistical Analysis

Statistical analyses were performed using GraphPad Prism 10. Results are expressed as mean ± standard deviation from at least three independent experiments. Statistical differences were analyzed by Student's unpaired t-test and One-way ANOVA followed by post-hoc Tukey's test, when appropriate. $p<0.05$ was considered statistically significant.

ANTIBODY	SUPPLIER	CATALOG #	DILUTION	APPLICATION
C-Myc	Cell Signaling	9402	1:1000 (WB) 1:100 (IHC)	WB, IHC
Actin	Sigma Aldrich	A5441	1:10000	WB
Vinculin	Santa Cruz Biotechnology	sc-73614	1:10000	WB
P62	Cell Signaling	5114	1:1000	WB
Ki67	Pierce	MA5-14520	1:100	IHC
ERK	Cell Signaling	9101	1:1000	WB
phospho-ERK	Cell Signaling	9102	1:1000	WB
GAPDH	Santa Cruz Biotechnology	sc-32233	1:10000	WB
Goat anti-Mouse HRP Conjugate	Bethyl	A90-116P	1:10000	WB
Donkey anti-Rabbit HRP Conjugate	Bethyl	A120-108P	1:10000	WB

Table 1. Antibodies, dilutions, and applications used. WB: Western Blot; IHC: Immunohistochemistry.

Name	Sequence 5' to 3'	Application
ACTIN_FW	CACCATTGGCAATGAGCGGTTC	qPCR
ACTIN_RV	AGGTCTTTGCGGATGTCCACGT	qPCR
LAMP1_FW	AGTGGCCCTAAGAACATGACC	qPCR
LAMP1_RV	AGTGTATGTCCTCTTCCAAAAGC	qPCR
TFE3_FW	GATCATCAGCCTGGAGTCCAGT	qPCR
TFE3_RV	AGCAGATTCCCTGACACAGGCA	qPCR
P62_FW	TGCCCAGACTACGACTTGTG	qPCR
P62_RV	AGTGTCCGTGTTTCACCTTCC	qPCR
EIF4G1_FW	TTGTGGATGATGGTGGCT	qPCR
EIF4G1_RV	TTATCTGTGCTTTCTGTGGGT	qPCR
EIF4A1_FW	CAACTATGACCTTCCC	qPCR
EIF4A1_RV	TGAGGTCAGCAACATTGAGG	qPCR
EIF4E1_FW	ACGGAATCTAATCAGGAG	qPCR
EIF4E1_RV	CCCACATAGGCTCAATAC	qPCR
PIK3CA_FW	GAAGCACCTGAATAGGCAAGTCG	qPCR
PIK3CA_RV	GAGCATCCATGAAATCTGGTCGC	qPCR
SPIKE_FW	GGATTAGGATCGTCGTAGTTAG	qPCR
SPIKE_RV	TAGCAGCAATCATAAAGCCC	qPCR
MYC_FW	CACCACCAGCAGGCACTC	qPCR
MYC_RV	TTCCACAGAAACAACATC	qPCR
mTOR_FW	TTCCGACCTTCTGCCTTCAC	qPCR
mTOR_RV	CCACAGAAAGTAGCCCCAGG	qPCR
EIF4G1	GCAGATAGTATCCAACACGTT	shRNA
EIF4A1	GCCGTAAAGGTGTGGCTATTA	shRNA
EIF4E1	CGGCTGATCTCCAAGTTTGAT	shRNA
mTOR	GCTGTGCTACACTACAAACCAT	shRNA
PIK3CA	GAATTGGAGATCGTCACAATA	shRNA
MYC	CCTGAGACAGATCAGCAACAA	shRNA
IRES_SG_UPSTREAM	AGTATAAAAGCCGGTTTTCG	sgRNA
IRES_SG_DOWNSTREAM	GCGACTCTCCCGACGCGGGG	sgRNA
SCR_SG	GCACTACCAGAGCTAACTCA	sgRNA
IRES_FW	CCCACCCTCCCCATAAGCG	PCR Screening
IRES_RV	GGAATGGGAGAAAAGACACCCT	PCR Screening

Table 2. DNA oligonucleotides used and their applications. All oligonucleotides were obtained from Bio-Fab Research. FW: Forward; RVL Reverse; qPCR: Quantitative PCR; sg: short guide RNA; shRNA: small hairpin RNA.

RESULTS

Chapter 1. Removal of the MYC IRES in does not affect MYC content in colon cancer .

We began our investigation into the role of the MYC IRES by utilizing the CRISPR/Cas9 gene editing system[93] to genetically remove this sequence from colorectal cancer cells. The MYC IRES spans from -94 to -363 bases upstream the noncanonical CUG start codon[83]. Primers for sgRNA are listed in Table 2. We validated the successful excision of this region of the MYC 5' UTR via PCR and sequencing (Figure 1A).

To determine if the removal of this region would affect basal levels of MYC protein content, we performed western blot in HCT116 and SW620 cells. With careful consideration that the MYC IRES is suggested to facilitate translation, we observed no difference in protein content between SCR (control) and ΔIRES (cells without the MYC IRES) cells in both cell lines (Figure 1B).

The MYC IRES overlaps with the P2 proximal promoter of MYC in a genomic context[83]. We hypothesized that removing the promoter that contributes ~75% of MYC mRNA content in cells[36] would deleteriously affect the levels of MYC mRNA in our ΔIRES cells. Remarkably, there appeared to be no

significant change in total MYC mRNA (Figure 1C), possibly due to compensation from the P1 promoter, as previously suggested[36].

Continuing with the careful investigation into biological effect of removing the MYC IRES, we performed polysomal fractionation experiments on SCR and ΔIRES cells to observe if there was a decreased association between ribosomes and MYC mRNA. Our data were normalized to a synthetic RNA (1 ng) that was injected into the system immediately before RNA extraction. We observed no difference in association between MYC mRNA and the different polysomal distributions, corrected for total mRNA variability across samples (Figure 1D, Figure 1E).

In summary, by removing the IRES region of CRC cells, we observe no change in MYC protein, mRNA, total mRNA, nor association to polysomes under basal cell culture conditions (for cell culture conditions, see Materials and Methods).

Chapter 2. Translation in the context of cap-dependent translation interference.

The next step in our investigation was to test the role of the MYC IRES through interfering the expression of critical components of the EIF4F cap-initiation complex. This complex plays a fundamental role binding mRNA to

the 40S ribosomal subunits, and is comprised of three main components: eIF4E, eIF4G, and eIF4A. We hypothesized that if the MYC IRES facilitates cap-independent translation, these critical components of the cap-initiation complex would not be necessary to maintain MYC protein levels. By definition, cellular IRES elements do not require eIF4E to initiate translation. However, they have been shown to have varying requirements for different components of the cap-initiation complex[67]. In particular, eIF4A, a helicase that unwinds RNA[94] has been suggested to be the critical cap-initiation factor for the MYC mRNA[95]. In addition to eIF4A and eIF4E, we interfered the expression eIF4G, a “scaffolding” protein that interacts with many components of the cap-initiation complex and is critical for creating the mRNA “loop” with the poly-A binding protein[96].

We first tested small-hairpin (sh)-mediated interference of eIF4E, the cap-binding protein. Validating successful interference via qPCR, we observed no rescue of the MYC protein content in SCR cells compared to ΔIRES cells in both HCT116 and SW620 cell lines (Figure 2A). Next, we investigated this response in cells interfered for eIF4G, the scaffolding protein. Upon validating successful small-hairpin interference via qPCR, we observed no rescue of MYC content in SCR cells compared to ΔIRES cells (Figure 2B). Testing last eIF4A, upon successful validation of small-hairpin interference, we again observed no rescue of the MYC protein in SCR cells

compared to ΔIRES cells (Figure 2C). The results here suggest that the MYC IRES does not facilitate MYC protein expression in conditions in which the canonical cap-dependent translation proteins are significantly reduced in cells.

Our next investigation was to test the activity of the MYC IRES using a luciferase assay technique that would bypass the issues that plague dicistronic DNA-based transfection experiments as well as dicistronic mRNA reporter experiments. To achieve this, we utilized *in vitro* transcription to transcribe monocistronic mRNA constructs, which then were to be transfected into cells. The design of the constructs is in Figure 2F. We designed four different constructs as follow:

1) The first construct simply contains a canonical 5' cap and luciferase mRNA.
2) The second construct contains a canonical 5' cap, followed by the MYC IRES, and followed by luciferase mRNA.
3) The third construct contains a synthetic cap (AP3G) that cannot be bound by eIF4E[97] followed directly by a luciferase mRNA.
4) The fourth construct contains the synthetic cap (AP3G), followed by the MYC IRES, and then a luciferase mRNA.

The hypothesis of this experiment is the following: if the MYC IRES facilitates internal ribosome entry, there would be a detectable expression of

the construct containing the synthetic cap, MYC IRES, and luciferase construct through the production of luciferase signal. A lack of signal could be due to either degradation of the mRNA or the IRES failing to initiate translation, therefore we performed quantitative PCR of the transfected construct to perform careful analysis. Cells were transfected as described (see Materials and Methods). After normalizing the luciferase results to the efficiency of their transfection, we observe no rescue of luciferase signal in the constructs containing the synthetic cap, MYC IRES, and Luciferase mRNA compared to our canonical 5' cap construct (Figure 2D).

We then finish our test of the MYC IRES in measuring proliferation in cells which contained interference for eIF4E. We hypothesized if MYC IRES facilitated cap-independent translation, there could be a rescue of cellular proliferation in cells that have interference for eIF4E. We however observed no such effect (Figure 2E), further suggesting the MYC IRES does not rescue cell proliferation when cap-dependent translation is inhibited.

As a summary for Chapter 2, we observed no rescue of the MYC protein in cells that have interference for the eIF4F cap-initiation complex. We observed no luciferase signal in cells transfected with the *in vitro* transcribed mRNA monocistronic reporter constructs containing the synthetic cap, MYC IRES, and luciferase mRNA. Also, we observed no rescue of cellular proliferation in cells with interference with eIF4E. Taken together, these

results suggest that the MYC IRES region does not facilitate cap-independent translation when canonical, cap-dependent translation is inhibited.

Chapter 3. Testing MYC content and cell viability in response to various cell stressors in colorectal cancer cells lacking the MYC IRES.

Based on previous works, we hypothesized that the MYC IRES could play a fundamental role in facilitating resistance to various stressors. Our investigation began with endoplasmic reticulum (ER) stress, a stress that the MYC IRES has been identified to provide responses that enable MYC translation. In multiple myeloma cells[98] MYC translation is enhanced in response to inducers ER stress, such as thapsigargin. Our results agree with some of their findings, as we observe a robust increase in MYC protein content upon treatment with 0.5 μM thapsigargin for 24 hours. However, our follow-up testing provides results that differ from their interpretation, as this induction is *not* IRES-dependent translation, as shown by the elevated MYC protein content observable in our ΔIRES cells (Figure 3A). We next wanted to determine which mechanism is responsible for this enhancement of MYC. By treating cells with both cycloheximide, an inhibitor of protein synthesis,

alongside thapsigargin, we could observe if this were due to increased stability or translation of the protein. As shown in Figure 3B, the enhancement of MYC in response to treatment with thapsigargin is completely ablated when co-treated with cycloheximide, a result that informed us the induction of MYC in response to the ER stressor was translational enhancement. This was an interesting phenomenon, considering multiple myeloma cells can resolve ER stress by inhibiting mTORC1 activity[99], and such survival mechanisms were previously attributed to the MYC IRES itself. Our results are in contrast with this attribution, as the IRES appears to play a role in no response to ER stress. To further address this, we wished to observe what would happen when we removed eIF4E from cells and then treated them with thapsigargin. We hypothesize that MYC mRNA should continue to translate if the IRES does indeed function for internal ribosome entry. The results of this experiment are presented in Figure 3C. With small hairpin-mediated interference of eIF4E, the enhancement of MYC mediated by treatment with thapsigargin is abrogated. These results suggest that the enhancement of MYC is due to increased cap-dependent initiation of translation.

We then wished to investigate if ΔIRES cells treated with thapsigargin would demonstrate reduced proliferation. As the MYC IRES was hypothesized to mediate cell survival in response to ER stress (referenced above), we would theoretically observe a rescue of cellular proliferation in

cells that contain the MYC IRES compared to those without it. As shown in Figure 3D, SCR and ΔIRES cells treated with thapsigargin showed a similar reduction in proliferation, with no statistical difference between the two. Taken together, our results indicate that the MYC IRES does not play a role in MYC translational enhancement in response to thapsigargin-mediated ER stress, nor does it play a role in facilitating cell survival to said stress.

The next step in the investigation was into the effects of genotoxic stress on cell proliferation and MYC expression. It has been proposed that the MYC IRES mediates translation during periods of genotoxic stress to maintain MYC cellular content and maintain the viability of cancer cells[100]. To address these claims, we utilized doxorubicin and 5-fluorouracil (5-FU), therapeutics that damage DNA, interfere with DNA replication, and cause significant cellular stress[101,102]. As shown in Figure 3E and Figure 3F, treatment with both doxorubicin and 5-FU, respectively, reduced but did not result in a complete loss of MYC protein content in colorectal cancer cells. However, the presence of the IRES in SCR cells did not affect the cellular content of the protein in comparison to ΔIRES cells that do not contain the MYC IRES.

We then investigated whether the IRES would promote cell survival in response to these compounds. Cellular proliferation was measured at 72 hours, and the results are presented in Figure 3G and Figure 3H for

treatment with doxorubicin and 5-FU, respectively. At none of the doses tested for both doxorubicin and 5-FU was there a rescue of cellular proliferation in control cells compared to ΔIRES cells.

Taken together, our results indicate that the MYC IRES neither facilitates translation of MYC, nor facilities cell survival during periods of genotoxic events.

It has been hypothesized that the MYC IRES can both facilitate MYC expression and enhance tumoral growth despite the metabolic hostilities of the tumor microenvironment, characterized by poor vascularization and low availability of nutrients and/or increased ROS production due to increased energy demand and consequent enhancement of mitochondrial metabolism[103]. Therefore, the next stresses we chose to investigate were characteristics of the tumor microenvironment that colorectal cancer cells experience: nutrient and oxidative.

To address nutrient stress, we utilized 2-deoxy-(2)-glucose (2DG), a glucose analogue that is not metabolizable and inhibits glycolysis, a key source of energy in most cancer cells[104]. As presented in Figure 3I, treatment with 2DG induces MYC protein expression. However, this occurs in both SCR and ΔIRES cells, suggesting the response is not an IRES-mediated mechanism. To further probe whether this response was indeed a cap-dependent translational mechanism, we used small hairpin interference to

knock down the expression of eIF4E and subsequently treated cells with 2DG. The ablation of eIF4E fully prevented the enhancement of MYC protein levels, further suggesting this response is indeed a cap-dependent mechanism (Figure 3J). Likewise, when we measured cellular proliferation in cells treated with 2DG, there was no rescue of SCR cells that contain the MYC IRES in comparison to ΔIRES cells that lack it, continuing to suggest the MYC IRES does not facilitate the MYC inductive-response to the metabolic stress caused by 2DG (Figure 3K).

In order to test the effects of oxidative stress, we utilized hydrogen peroxide. Similarly to the effect of 2DG, the use of H_2O_2 induced MYC expression in both SCR and ΔIRES cells, suggesting the enhancement is not due to IRES-mediated translation (Figure 3L). When we attempted to confirm this effect was due to cap-dependent translation be interfering with the expression of eIF4E in HCT116 cells, we interestingly observed that the levels of MYC were still elevated, as shown in Figure 3M. It is known that MYC phosphorylation at S62, an effect caused by H_2O_2, prevents it from being recognized and engaged by the proteasome[105]. We therefore hypothesized that the enhancement we observe could be due to increased protein stability rather than increased protein translation. By treatment of cells with both H_2O_2 and cycloheximide, we continued to observe an enhancement of MYC in the dual-treatment condition (Figure 3O). This result suggests the

enhancement of MYC in response to oxidative stress is independent of changes in translation and is instead mediated by a mechanism of enhanced stability. Finally, we wanted to observe if the presence of the MYC IRES would allow for any enhancement of cell proliferation to oxidative stress. In line with our other results, the presence of the MYC IRES in control cells did not rescue their proliferation when compared to the proliferation of cells without the IRES (Figure 3N).

Together, these data demonstrate that the MYC IRES does not facilitates survival mechanisms engaged by tumoral cells in the tumor microenvironment to survive stresses.

Chapter 4. The MYC proximal promoter enhances transcription in response to PI3K inhibition.

PI3K signaling is a critical intracellular pathway that regulates a variety of cellular processes including development, metabolism, growth, and motility[106]. A fundamental role for PI3K in colorectal cancer was found when mice knocked out the gamma catalytic subunit of PI3K developed carcinoma[107]. Likewise, publicly available datasets show PIK3CA mutations are one of the more commonly observed molecular changes in colorectal

cancer[108,109]; these data together present PI3K as an attractive target for cancer therapy.

Promisingly, a direct role on MYC protein content has been established by PI3K activation via phosphorylating and increased proteolytic degradation of the MYC antagonist Mad1[110], and is known to influence activity at the MYC promoter through a variety of pathways[36]. However, MYC overexpression has been linked to a number of cancer therapies with a critical role of mediating chemoresistance[111–113]. The complexities of the MYC promoter allow it to facilitate numerous cross-regulatory signals and at times allow the cells to cope with conflicting input.

Efforts to inhibit PI3K has led to unexpected results. Contrary to expectations, the dual mTOR/Pi3K inhibitor BEZ235 was found to increase cellular MYC translation, an effect attributed to the presence of the IRES region[46]. We were curious if cells lacking the MYC IRES would demonstrate loss of translational enhancement in response to dual mTOR/PI3K inhibition. As shown in Figure 4A, our results of a 24-hour treatment with BEZ235 are in agreement with Wiegering et al. 2015[46], as our SCR control cells with the intact IRES demonstrated the dose-dependent induction of MYC protein content in response to BEZ235. However, this response was not observed in our ΔIRES cells. We then utilized knockdown of eIF4E to test if this enhancement was mediated by cap-independent initiation of translation, as

suggested by the authors. However, as shown in Figure 4B, the induction of MYC via BEZ235 treatment is completely abrogated with the interference of eIF4E, suggesting this response is a cap-dependent mechanism but still reliant on the IRES region of MYC. Intrigued by these results, we wished to specify whether the response of MYC induction via BEZ235 could be attributed to mTOR or PI3K alone. By utilizing small-hairpin mediated interference for both targets, knockdown of mTOR demonstrated no induction of MYC protein content in neither SCR nor ΔIRES cells (Figure 4C), while we found that interference with PIK3CA induced MYC expression in SCR cells but not ΔIRES cells (Figure 4D). Figure 4E and Figure 4F shows the knockdown efficiency of TOR and PIK3CA, respectively. We then attempted to repeat this response with the clinically tested, selective pan-acting class I Pi3K inhibitor, BKM120[114]. Figure 4G shows the representative results of 24-hour treatments of BKM120 in SCR and ΔIRES cells. A dose-dependent induction was observed, and indicated the response MYC to these compounds is indeed due to PI3K inhibition.

As we observed an enhancement of MYC protein content in SCR cells but not ΔIRES, we were curious if this enhancement via BKM120 was a cap-dependent induction similar to that of BEZ235. To test this hypothesis, we utilized small hairpin mediated interference of eIF4E alongside treatment of BKM120. We observed that interference with eIF4E prevented the induction

of MYC protein (Figure 4H), suggesting this response is in fact a cap-dependent mechanism, and because there is a complete abrogation of the induction, the results also show the induction of MYC is not due to increased stability of the protein. To both focus specifically on the mechanisms of PI3K inhibition on MYC induction, and to minimize off-target effects of BEZ235 in our study, we continued our investigation solely using BKM120 as opposed to BEZ235.

Thus far, the results indicate the MYC induction in response to PI3K inhibition is a cap-dependent mechanism while still reliant on the MYC IRES, a mechanism we were curious to understand. Wiegering et al. 2015 demonstrated that by using silvestrol, an inhibitor of eIF4A[115], association of MYC mRNA to polysomes was inhibited by ~75%[46]. This response was reasoned to be due to the critical role of eIF4A functioning as a translational initiation factor for the MYC IRES[95]. We wondered if our ΔIRES cells would demonstrate this same reduction with PI3K inhibition. We performed polysomal fractionation experiments in SCR and ΔIRES cells treated with BKM120 [1 μM] for 24 hours and found a decrease in global translation in both SCR and ΔIRES cells (Figure 4I). One representative experiment is shown with a decrease of translation efficiency for SCR and ΔIRES cells to 67.14% and 67.83%, respectively, when treated with BKM120. Interestingly, upon analysis of the association of MYC mRNA to polysomes, Two-way

ANOVA yielded no significant difference in the between treatments of DMSO vs. BKM120 in all fractions (Figure 4J, Figure 4K), suggesting that PI3K inhibition does not readily affect association of MYC mRNA to polysomes in colorectal cancer cells. Importantly, the MYC IRES was not critical for maintaining MYC translation in these conditions. We therefore could not attribute the enhancement of MYC protein content in SCR cells treated to an increased rate of translation - neither canonical nor cap-independently initiated mechanisms.

From our results in this chapter thus far, we reasoned (1) the enhancement of MYC protein in response to PI3K inhibition cannot be attributed to internal ribosome entry into MYC mRNA, and (2) the results cannot be attributed to translational enhancement. Therefore, we hypothesized it must be due to an alteration of MYC mRNA content, either its biosynthesis or turnover.

In order to investigate the hypothesis that BKM120 could be impacting the rate of MYC mRNA turnover, we treated our SCR (Figure 4L) and ΔIRES synthesis inhibitor actinomycin D [5 μg/mL] for the indicated time points. Analysis of MYC mRNA demonstrated no difference in its half-life between in both SCR and ΔIRES cells treated with BKM120 compared to controls. We then ruled out the possibility that PI3K inhibition is affecting the stability of MYC mRNA.

We then investigated if treatment with BKM120 would induce MYC mRNA expression. Interestingly, by quantitative RT-PCR, we observed that BKM120 caused a significant increase in MYC mRNA in SCR cells as opposed to ΔIRES cells (Figure 4N). Our results indicate that BKM120-mediated PI3K inhibition results in a transcriptional increase of MYC expression that involves the IRES region of the MYC locus in a genomic context.

A previous study suggested that the induction of MYC protein content from dual mTOR/PI3K inhibition could be attributed to increased activity at the MAP kinase pathway functioning on the joint E2F/ETS promoter element in MYC[46]. In order to test if this pathway was active in our model, we treated SCR and ΔIRES cells with the MEK inhibitor U0216[116,117]. We found that the enhancement of MYC in SCR cells via BKM120 was completely abrogated with co-treatment treatment of U0216 [0.5 μM] for 24 hours (Figure 4O), and we concluded that the inhibition of PI3K specifically is mediating an enhancement of MYC through MEK signaling, in further consistency with the previous results[46].

The MYC IRES exists at the terminal 5' end of exon 1 in MYC. This coincides with P2 promoter, which starts on the same nucleotide. However, they do not share the same length, as the length of IRES is 269 bases, extending beyond the 3' end of the P2 promoter. We were curious to test if

the rest of the IRES region could contribute to the observed transcriptional enhancement of MYC in response to PI3K inhibition. To this effort, we designed an HBM-IRES-Luciferase construct based on the published MYC promoter reporter construct HBM-Luciferase[118]. This construct contains the MYC promoter, originally cloned from the MYC locus at a HindIII restriction site 2052 bases upstream relative to the P2 promoter. In this construct, without introducing any extra nucleotides, we included the remainder of the IRES sequence to the 3' terminal end of the P2 promoter. In this way, when treated with BKM120, we can detect if there is an enhancement of luciferase signal by comparison to the construct without the IRES 3' extension as compared to just the P2 promoter itself. The reporter construct designs are visualized in Figure 4P (image created in BioRender). By transfecting these reporter constructs and treatment with either DMSO or BKM120 [1 μM] for 24 hours, we observed a significant increase in luciferase activity of the HBM-IRES-Luciferase construct compared to the HBM-Luciferase construct alone when treated with BKM120 (Figure 4Q). This result suggests the MYC IRES plays a critical role in the transcriptional responses to PI3K inhibition in addition to MEK signaling.

Collectively, these results indicate that rather than functioning at the translational level, BKM120-mediated inhibition of PI3K affects the

transcription of MYC in a mechanism both relying on the IRES sequence in a genomic context, and MEK signaling.

Chapter 5. The loss of the MYC IRES abrogates resistance to PI3K inhibitors *in vitro* and in mice.

After observing the MYC IRES playing a role in the upregulation of MYC in response to PI3K inhibition, we were curious to observe if this effect could be playing a role in the resistance of class I PI3K inhibitors in CRC cells[119–121]. By treatment of SCR and ΔIRES cells with BKM120 [0.5 μM] for three days and measuring their proliferation, we observed an anti-proliferative sensitivity of ΔIRES cells to BKM120 compared to SCR control (Figure 5A). This result suggests that the IRES region of MYC could play a role in the sensitivity of CRC cells to class I PI3K pharmacological inhibition.

We wanted to validate this pathophysiological finding *in vivo*. To achieve this, we measured the growth of grafted HCT116 SCR and ΔIRES cells in the flanks of nude mice (2.0×10^6 cells/flank). Once the tumors reached a volume of 100 mm^3, mice were treated with BKM120 (30 mg/mL)

in a vehicle of 90% corn oil/10% DMSO[1] daily via oral gavage for 15 days. Every 3 days the volume of each tumor was recorded. At 15 days, the mice were sacrificed, tumors were removed, weighed, and photographs as well as samples for molecular analyses were collected. Figure 5B shows representative images of the SCR tumors and Figure 5C the growth of their volume over the 15-day period as measured by calipers. In Figure 5D, the representative images of ΔIRES cells and in Figure 5E the growth of their tumor volume over the 15-day period. Consistent with previous observations, there was a significant difference in the volume of the tumors in between the ΔIRES cells treated with BKM120 or vehicle, but not SCR cells treated with BKM120 or vehicle. Likewise, there is a significant difference in the tumor weight between ΔIRES cells treated with BKM120 versus control, and not SCR (Figure 5F). Moreover, we did not observe a difference in the immunohistochemical staining for Ki67 between SCR treated with BKM120 and vehicle but did for ΔIRES cells treated with BKM120 and vehicle, confirming the antiproliferative effect of BKM120 in ΔIRES cells occurs also *in vivo* (Figure 5G). We observed an increase in immunohistochemical staining for MYC in SCR xenografted cells treated with BKM120 compared to SCR

[1]. DMSO in this formulation served as a solvent for BKM120. DMSO administered orally to mice presents low acute toxicity[122]

controls, and no increase in ΔIRES xenografted cells treated with BKM120. We found the upregulation of MYC via PI3K inhibition was validated in tumor samples collected by western blot for MYC protein (Figure 5H) both quantitative RT-PCR for MYC mRNA (Figure 5I).

The results presented in this chapter suggest that the antiproliferative effects of BKM120 exhibited by ΔIRES cells also occurs *in vivo*, providing translational evidence where cellular conditions are significantly more heterogenous, as typical of a tumor microenvironment. This can involve differences in oxygen within the tumor, as well as pH, and nutrient availability.

Chapter 6. The resistance of CRC cells to PI3K inhibition is linked to MYC-mediated induction of autophagy.

We next desired to understand the mechanism in which colorectal cancer cells were exhibiting resistance to PI3K inhibition. It has been previously demonstrated that MYC alone is capable of providing resistance to mTOR inhibition[123], and that MYC activates resistance to conventional chemotherapy through activation of the oncogenic stress[124]. Pervious works specifically with PI3K inhibitors have unveiled their ability to induce autophagy[125], and considering that MYC is an important driver of

autophagosome formation[126], we wondered if the MYC IRES region could be modulating this effect.

Our first experiment was to stain our HCT116 SCR and ΔIRES cells with LysoTracker Red (ThermoFisher #L7528), a dye that visualizes acidic compartments in living cells. After counterstaining with DAPI and confocal microscopy, we interestingly found there is an enhancement of the LysoTracker Red signal in the SCR cells, but not the ΔIRES cells treated with BKM120 [1 μM] for 24 hours (Figure 6A). The results suggest that PI3K inhibition is promoting the formation of acidic content. However, on its own, this result does not strictly dictate an increase in the autophagic flux. Therefore, to confirm a change in the formation of autolysosomes in response to PI3K inhibition, we utilizes the tandem reporter construct mCherry-GFP-LC3B[127] (AddGene #124974). This construct, containing the LC3B protein, visualizes itself as yellow when both GFP and mCherry fluorescence signals are detected and overlapping. The loss of the green GFP signal indicates exposure of the GFP to acidic content[127]. This occurs when LC3B is converted from I to II during autophagosome formation and its conjugation to phosphatidylethanolamine[128]; therefore when LC3 is integrated into autophagosomes, only the mCherry signal will be detected. We tested whether there would be a difference between red vs yellow signal in SCR and ΔIRES cells constitutively expressing the mCherry-GFP-LC3B reporter

treated with BKM120 [1 μM] for 24 hours (Figure 6B). We observed SCR cells demonstrate a strong transition to red signal after treatment with BKM120, indicating a transition towards producing autophagosomes. ΔIRES cells, contrary to SCR cells, exhibit little-to-no increase in the red signal. Bafilomycin A, an inhibitor of autophagy, was used as a control. These results strongly indicate that there is an increase in conversion of LC3B I to II, and that autophagosome formation is elevated as a response to BKM120 and PI3K inhibition, and that this response requires the MYC IRES.

To confirm an increase in autophagic flux after autophagosome formation, we tested whether P62 degradation would be consistent with our results. P62, also known as sequestosome-1, is a component of the autophagosome and is degraded in an autophagic mechanism; it therefore is conveniently used to monitor changes in the autophagic flux[129]. We hypothesized that SCR cells, as they demonstrate an increase in LC3B II to I conversion in response to PI3K inhibition, would yield a decrease in P62 signal, but not in the ΔIRES cells. Upon BKM120 treatment [1 μM] for 24 hours, our hypothesis was confirmed, as we observed a consistent reduction in P62 protein in SCR cells compared to ΔIRES cells (Figure 6C). The results were quantified via densitometry, yielding a significant decrease in P62 optical density in SCR cells treated with BKM120 compared to ΔIRES cells (Figure 6D). To confirm this response was not due to transcriptional changes

in P62 expression, we simultaneously performed quantitative RT-PCR and found treatment the BKM120 did not negatively affect the transcription of P62 (Figure 6E).

Mechanistically, MYC is known to be a critical component of autophagosome formation[126]. We found that two genes involved with lysosome biogenesis and induction of autophagy, LAMP1 and TFE3, respectively, were signficantly upregulated in SCR cells treated with BKM120, and not ΔIRES cells (Figure 6F, Figure 6G). To further validate this mechanism and a specific role for MYC, we interfered with the expression of MYC using small-hairpin RNA. Upon MYC knockdown followed by treatment with BKM120 for 24 hours, we found that the induction of acidic content was completely abrogated, as visualized by LysoTracker Red (Figure 6H). Furthermore, the reduction of P62 levels in response to BKM120 treatment was inhibited when MYC was knocked down (Figure 6I).

We then investigated the combination effect of BKM120 and Bafilomycin A on the proliferation of SCR and ΔIRES cells. We hypothesized that if the MYC IRES were to play a role in facilitating the autophagic response, we could potentially observe a combination effect between PI3K inhibition and inhibition of the autophagic flux in our control SCR cells, but no combination effect in the ΔIRES cells. To test for this, we utilized a low dose of Bafilomycin A [2 nM] to minimize its specific effects on proliferation and

analyzed the relative proliferation via one-way ANOVA (n=4, $p<0.05$) followed by Tukey's post hoc test. Significance asterisks in the figures represent the post-hoc test, relative to DMSO. Consistent with our previous experiments, upon treatment with BKM120 alone, we found no decrease in cellular proliferation in SCR cells treated with BKM120 [0.5 μM], and a significant reduction in ΔIRES cells (Figure 6J, Figure 6K). SCR cells treated with Bafilomycin A exhibited no reduction in cellular proliferation, whereas ΔIRES cells demonstrated a reduction, suggesting a sensitivity of these cells to inhibitors of autophagic inhibitors. Most interestingly, there was a significant reduction of proliferation in SCR cells treated with both BKM120 and Bafilomycin A, supporting the notion that the resistance to BKM120 and PI3K inhibition are indeed linked to induction of autophagy. Further, we found no combination effect with this dual treatment in our ΔIRES cells, solidifying the hypothesis that the MYC IRES plays a role in the induction of the autophagic flux as an adaptive response to PI3K inhibition.

The results presented in this chapter suggest the MYC IRES plays a role in the autophagic response of colorectal cancer cells to PI3K inhibition. Specifically, the enhancement of MYC increases the amount of autophagosomes, which leads to an increased rate of the autophagic flux, a process that mediates the resistance to Pi3K inhibitors.

Chapter 7. Specific translocations of sporadic MYC in Burkitt Lymphoma cells demonstrate increased sensitivity to PI3K inhibtion.

Burkitt Lymphoma (BL) is a non-Hodgkin B-cell lymphoma cytogenically characterized by a translocation of the MYC oncogene to an immunoglobulin promoter element. In particular, a MYC/IGH translocation t(8;14)(q24;q32) occurs in ~80% of cases[130], placing MYC under the transcritpional regulation of the IGH promoter. The other two variants, t(2;8)(p12;q24) and t(8;22)(q24;q11) occur on the IGK and IGΛ loci, respectively, account for the remaining ~20% of cases[131]. This translocated MYC gene is highly expressed while the normal allele is either silent or expressed at low levels, a common finding among all Burkitt Lymphoma cells[132,133].

In many cases of BL, some or all of the regulatory elements of the MYC promoter are translocated in addition to the coding region, which could potentially subject dysregulate MYC signaling. Burkitt Lymphoma is clinically categorized into variants that correlate with the location of the MYC breakpoints: The first variant is known as endemic BL. Endemic BL is typically found in regions of Africa, and associated with malaria infection alongside Epstein-Barr Virus infection[134]. In endemic BL, the MYC oncogene is generally translocated 5' outside the MYC locus, leaving the translocated gene and its regulatory elements intact[135–137]. The second variant is sporadic,

and is found within the rest of the world, typically in North America and Europe[134]. In cases of sporadic BL, the most common site of the MYC translocation is within the MYC locus, particularly within intron 1 or exon 1[138]. The third variant is immunodeficient, and typically associated with HIV[139], whose correlation with the translocation breakpoint of MYC is not well characterized.

Interestingly, the nature of the translocation site in sporadic BL effectively dissociates either partially or all of exon 1 from the translocated portion of MYC, and by extension, the MYC IRES region. This translocated MYC could then fail to respond to upstream signaling pathways. We hypothesized that BL cells with this type of translocatin could exhibit a similar response as our ΔIRES cells to PI3K inhibition via BKM120 treatment. Specifically, we were interested if BL cells lacking the IRES with PI3K inhibited by BKM120 would demonstrate sensitivity, both by an antiproliferative response and a lack of autophagic induction, when compared to BL cells whose regulatory regions were translocated intact. To this goal, we utilized two BL cell lines – Raji, which contain a fully translocated gene[140], and DG75, a cell line which contain the translocation dissociating the MYC IRES from the translocated portion of MYC[141] (Figure 7A).

To test if the IRES region would play a role in the induction of MYC also in these cells, Raji and DG75 cells treated with BKM120 [1 μM] for 24 hours.

Western blot analysis revelaled Raji cells had elevated MYC protein content when treated with BKM120, whereas DG75 cells did not (Figure 7B), confirming our hypothesis. Excited by these results, we were curious if the same in autophagic flux would be observed in a similar pattern as HCT116 SCR/ΔIRES cells. Raji cells treated with BKM120 and subsequently stained with LysoTracker Red demonstrated a robust increase in acidic content while DG75 cells demonstrated no induction (Figure 7C). Confirming an increase in the autophagic flux, Raji cells yielded decreased P62 protein content after BKM120 treatment whereas whereas DG75 cells did not (Figure 7B). This effect was significantly quantified via densitometry (Figure 7D). Continuing in this investigation, we found by using our tandem reporter mCherry-GFP-LC3B, there was a conversion of the yellow (lysosomal) to red (autophagosome) signal in the Raji cells treated with BKM120, but not the DG75 cells (Figure 7E). Similarly to the response in HCT116 SCR and ΔIRES cells, Raji cells demonstrated an increased transcriptional expression of LAMP1 and TFE3, respectively, when treated with BKM120, while DG75 cells failed to do so (Figure 7F, Figure 7G).

These results taken all together suggest that the IRES portion of the MYC locus, absent in the translocated MYC in the Burkitt Lymphoma cell line DG75, is critical for the induction of the autophagic flux in response to BKM120 treatment not only in colorectal cancer cells but also Burkitt

Lymphoma cells. Confirmed a role for MYC, interference for MYC via shRNA yielded an ablation of the induction of acidic content in Raji cells when treated with BKM120 (Figure 7H).

We then examined the effects of dual BKM120 and Bafilomycin A on cellular proliferation to observe a synergistic response between PI3K inhibition and inhibition of the autophagic flux. We hypothesized that, similarly to the mechanism delineated with HCT116 cells, that Raji cells would demonstrate a decreased sensitivity to BKM120 and a synergistic antiproliferative effect in the dual treatment of BKM120 and bafilomycin A. In addition, we hypothesized DG75 cells would be sensitive to BKM120 and not demonstrate a combination response. Cells were treated for 7 days with BKM120 [0.1 μM] and/or bafilomycin A [0.4 nM]. The results are presented in Figure 7I and Figure 7J. Significance asterisks refer to Tukey's post-hoc test relative to DMSO, which was preceded by one-way ANOVA ($n=3$, $p<0.01$ in both cell lines). Raji cells demonstrated no significant antiproliferative sensitivity to BKM120 treatment, similarly to HCT116 SCR cells, whereas DG75 cells were found demonstrate significant antiproliferative effects. When treated together with bafilomycin A and BKM120, there was an antiproliferative response for Raji cells, but no stronger effect than BKM120 alone was observed in DG75 cells, indicating that in the case of Burkitt

Lymphoma cells too, the IRES is critical for the induction of the autophagic flux to facilitate resistance to PI3K inhibitors.

Collectively, the results in this chapter demonstrate the MYC IRES plays a fundamental role in the resistance of not only colorectal cancer cells to PI3K inhibition, but other cancers as well, as demonstrated here with Burkitt Lymphoma cells. Raji cells shown here have a translocated MYC IRES and are able to exhibit a form of resistance to PI3K inhibition by inducing MYC and then both increasing autophagosome formation and the autophagic flux. Likewise, DG75 cells that lack the MYC IRES on the translocated MYC locus exhibit antiproliferative sensitivity to PI3K inhibition, and neither induce MYC in response to the inhibition, nor induce the increase in autophagic flux when compared to the observations in cells that do have the IRES sequence intact on the translocated MYC locus.

DISCUSSION

Protein translation is a highly regulated and energetically demanding process that contributes to several aspects of cell pathophysiology. Initiation of translation, its key regulated step, canonically requires a m7G cap-structure at the terminal 5’ end of mRNA. A cell is periodically exposed to harmful conditions during its life that require the prompt activation of compensatory and retaliatory mechanisms, which in part can aim to save energy while simultaneously fixing or alleviating the damage induced by the conditions themselves. In these types of conditions, global cap-dependent translation is usually inhibited to save energy while a subset of mRNAs encoding stress response proteins escape this repression to restore cell homeostasis.

The existence of the MYC IRES has been subject to a great deal of controversy for many years, and research regarding both its validity and absence have been published since the 1990s. In this thesis, a contribution to the body of evidence is presented using techniques incorporating the correct degree of sensitivity, as well as investigating more biologically relevant models in which cellular IRES elements are suggested to function. The results clearly indicate that the MYC IRES fails to facilitate the translation of MYC under a wide variety of cellular stresses. If the MYC IRES were to aid

translation in periods of cell stress, we would observe a maintainment of cellular MYC protein content or cellular proliferation rate, especially considering MYC facilitates the entry into the S-phase[142]. These hypotheses were not observed; on the contrary, all evidence consistently points towards the MYC IRES not facilitating any sort of response in any experiment probing IRES-mediated translational activity. We believe the types of techniques used to probe for cellular IRES activity should be highly controlled and the use of dicistronic reporter constructs avoided, for reasons previously presented[72], namely the production of monocistronic products due to unforeseen splicing events and cryptic promoters. Our lab as a whole dose not disagree with the premise of cellular IRES elements, as we have previously demonstrated the presence and functionality of an IRES in ODC1 mRNA[143] using similar methodology as presented in this thesis.

PI3K signaling regulates many aspects of cell survival, metabolism, and proliferation among other processes, and in particular via AKT/mTOR signaling[144]. Due to its implication in the development of colorectal cancer (see subsection Genes Implicit in Colorectal Cancer), many therapeutic approaches have been developed and tested clinically to treat numerous cancers. The first inhibitor, idelalisib (also known as Zydelig), which targets P110δ, was approved by the U.S. Food and Drug Administration (FDA) in July 2014 to treat chronic lymphocytic leukemia[145]. As of January 2024, there

are five other FDA-approved PI3K inhibitors: copanlisib[146], alpelisib[147], duvelisib[148], and umbralisib[149], though umbralisib approval was revoked for deleterious side effects. In any case, none of these PI3K inhibitors were approved for colorectal cancer therapy. Clinical trials of various stages using PI3K inhibitors alone and in combination for colorectal cancer have been completed or are ongoing (ClinicalTrials.gov identifiers: NCT01390818, NCT04495621, NCT01719380, NCT01068483). However, pan-acting PI3K-targeted inhibitors as a whole have had limited success in the clinic due to resistance to the inhibition that can be partially attributed to the downstream feedback mechanisms following PI3K inhibition[121]. Considering MYC plays a role in the chemotherapy-resistant response of many cancers[111–113], it is possible that MYC can contribute to the resistance of PI3K inhibitors, though research on this area is limited. Of note, we have found evidence that the MYC proximal promoter and IRES region in a genomic context play a pivotal role in the resistance to pan class I PI3K inhibition. Colorectal tumors that demonstrate genetic aberrations in the MYC locus, such as those undergoing CIN aneuploidy, could exhibit the ΔIRES phenotype that is susceptible to PI3K inhibition.

PI3K inhibition should significantly alter the activity of the PI3K/AKT/mTOR pathway. PI3K activity leads to the phosphorylation and activation of AKT[150]. Inversely, the inhibition of AKT caused by PI3K inhibition

should result in the phosphorylation of MYC at T58 by a dephosphorylated and activated GSK3β[151], and lead to the proteolytic degradation of MYC. Furthermore, mTORC1, which phosphorylates 4E-BP, is stimulated by PI3K activity[152] and translation could be inhibited by buparlisib-mediated PI3K inhibition. Likewise, PS6, an important protein in regulating the initiation of translation[153] translation too should decrease with mTORC1 inactivation[154]. Indeed, we observe a decrease in global translation during PI3K inhibition in both our SCR and ΔIRES cells. However, we observe an increase in MYC protein content in response to PI3K inhibition that cannot be attributed to increases in MYC stability, an observation in agreement with Wiegering et al., 2015[46]. These results, seemingly contradictory to the established pathway of PI3K/AKT/mTOR signaling, can be attributed both in part to the increase in MYC transcription mediated by FOXO3a and MAP kinase activity[46], and our interesting result that the association of MYC mRNA to polysomes is not altered during PI3K inhibition. Importantly, this association is completely independent of the IRES in MYC mRNA, suggesting an alternative mechanism of preferential mRNA translation.

As stated above, PI3K inhibition was shown rather to activate GSK3β and promote MYC degradation, it activates a FOXO3a-dependent activation of the MAP kinase pathway[46] that increases transcription of MYC via the dual ETS/E2F sequence in the MYC promoter[156]. Indeed, our results suggest this

same result through the use of the MEK inhibitor U0126 alongside BKM120. However, our results add more understanding to this induction, which is an in-tact IRES region of MYC is a requirement. This sequence, rather than facilitating internal ribosome entry, plays a role in the induction of MYC transcription perhaps because it harbors many potential transcription factor binding sites, and is known to be loaded with RNA polymerase II paused in the elongation phase of transcription[157,158] just ~30-300 bases downstream the P2 promoter[157,159]. RNA polymerase paused in the elongation phase allows for a rapid enhancement of MYC levels in response to particular stimuli[160–163] that quickly release the transcriptional block. Interestingly, this phenomenon is particularly responsive to E2F signaling[164]. it is possible that the block of transcriptional elongation is alleviated in response to PI3K inhibition through E2F activity, which then allows for the rapid transcription of MYC observed in SCR cells compared to ΔIRES cells. Our results suggest that in addition to inhibitors of autophagy, MEK inhibitors, such the FDA-approved trametinib[165], could function effectively at alleviating MYC-induced resistance to PI3K inhibitors by preventing its transcriptional enhancement.

Some proteins are preferentially translated during times of cell stress, and this could contribute to their role in chemoresistance, in particular, MYC[124]. Stress exposure to cells activates eIF2α via phosphorylation by it serving as a substrate for one of the four known protein kinases mediating its

activity[167]. eIF2α plays a key role in the initiation of eukaryotic translation by mediating the bind of the 40S ribosome subunit to a methionine-loaded tRNA. Phosphorylation of eIF2α leads to its inactivation (the PI3K inhibitor LY294002 has been shown to increase eIF2α phosphorylation in murine embryonic fibroblasts[168]). Paradoxically, when eIF2α is phosphorylated, specific mRNA are still translated, and some are translated at an even higher rate[52]. A common finding among these so-termed stress-response mRNA are they contain upstream open reading frames (uORFs)[169] that facilitate ribosome translation through the CDS when phosphorylated eIF2α levels are high. MYC coincidentally contains a uORF as it codes for a N-terminally extended protein initiating from an upstream non-canonical CUG start codon. This provides a potential mechanism for the maintainment of MYC protein content during times of stress that is not dependent on an IRES.

Another aspect of stress translation is mediated through transfer RNA (tRNA). During stress, transcription of tRNAs is generally inhibited, however, one class of tRNA genes do not change their expression profile[52], resulting in codon-biased translation[170–172]. Furthermore, translational fidelity (accuracy of codon:anticodon pairing) decreases the rate in which cells can produce proteins and grow; in essence, the more accurate translation is, the slower the process[52,173,174]. Miscoding during stress is promoted by tRNAs via cleavage[175,176], modification (such as methylation[177]) and the general

redundancy of codon pairing, allowing for sustained translation during stress, such as when eIF2α is phosphorylated. Mechanistically, these stress-related translational regulatory mechanisms can facilitate MYC translation when global protein translated is inhibited, in a cap-dependent manner, and without the need for internal ribosome entry.

Burkitt Lymphoma is considered the fastest growing human tumor[134] and accounts for 40% of the yearly diagnosed childhood non-Hodgkin's lymphoma in the United States of America[178]. The disease is a highly treatable malignancy, with over 90% of patients being cured[179] through multiagent chemotherapy, particularly in children. The sensitivity of Burkitt Lymphoma cells lacking the MYC IRES to PI3K inhibition in a genomic context is novel, and worth further investigation. Here, we have identified a sensitivity found in translocation-specific cases of Burkitt Lymphoma to PI3K inhibition. Mechanistically, we found that in instances the translocated MYC oncogene does not contain the regulatory MYC IRES, the cells cannot induce a MYC-dependent autophagic adaptation to the inhibition of PI3K, and subsequently suffer from a robust antiproliferative response.

Despite BL being a highly treatable disease, one investigation found children diagnosed as clinically high-risk (risk groups R3 and R4) have relapse rates exceeding 15%, and survival at relapse a mere 20%[180]. In the referenced investigation, the researchers studied the correlation between

occurrence and location of the breakpoint relative to the MYC locus. They found, in clinically high-risk children enrolled approved NHL-BFM study groups from 01/2000 to 02/2017, 44% had translocations within intron 1 or exon 1 of MYC[180]. These data could suggest that a significant proportion of children with the highest relapse rate of BL *and* with the lowest survival rates at relapse could potentially benefit from PI3K-targeted chemotherapy. Although PI3K inhibitors have been tested in different experimental paradigm for BL pre-clinically[181–183], as of January 2024, the use of PI3K inhibitors in a clinical trial of Burkitt Lymphoma has not been attempted. The results presented in this thesis suggest a potential applicability of PI3K inhibition in the treatment of Burkitt Lymphoma.

CONCLUSION

In conclusion, the results of this thesis demonstrate that the immediate 5’ region of MYC mRNA to the non-canonical CUG start codon does not contain an internal ribosome entry site. The results also suggest this region, identified historically as an IRES, neither facilitates the expression of MYC in response to a number of cell stresses nor does not it facilitate the survival of colorectal cancer cells to said stresses. Colorectal cancer cells with the MYC

IRES demonstrate resistance to PI3K inhibition via an autophagic adaptation mediated, at least in part, by MYC transcriptional activation.

Translation of MYC is maintained when global translation is reduced, mediated by a translational mechanism that does not require internal ribosome entry. Furthermore, colorectal cancer cells lacking the immediate 5' region of MYC mRNA demonstrate an inability to induce both MYC transcriptionally, an inability to increase the autophagic flux, and demonstrate an anti-proliferative vulnerability in response to pan class I PI3K inhibition. The activation of MYC is mediated via a signaling cascade by FOXO3a, activating MAP kinase signaling, and promoting transcription of MYC dependent on its immediate 5' region in a genomic context. The inability to induce MYC and its autophagic responses when treated with BKM120, resulting in the antiproliferative effect, is also observed in Burkitt Lymphoma cells whose translocated MYC oncogene does not contain MYC immediate 5' region. Clinically, these results present a potential mechanism of resistance to PI3K inhibition via MYC expression and suggest a novel application for chemotherapy targeting PI3K in sporadic Burkitt Lymphoma.

FIGURES

Figure 1. The deletion of the MYC IRES neither affects MYC protein nor mRNA content under basal conditions.

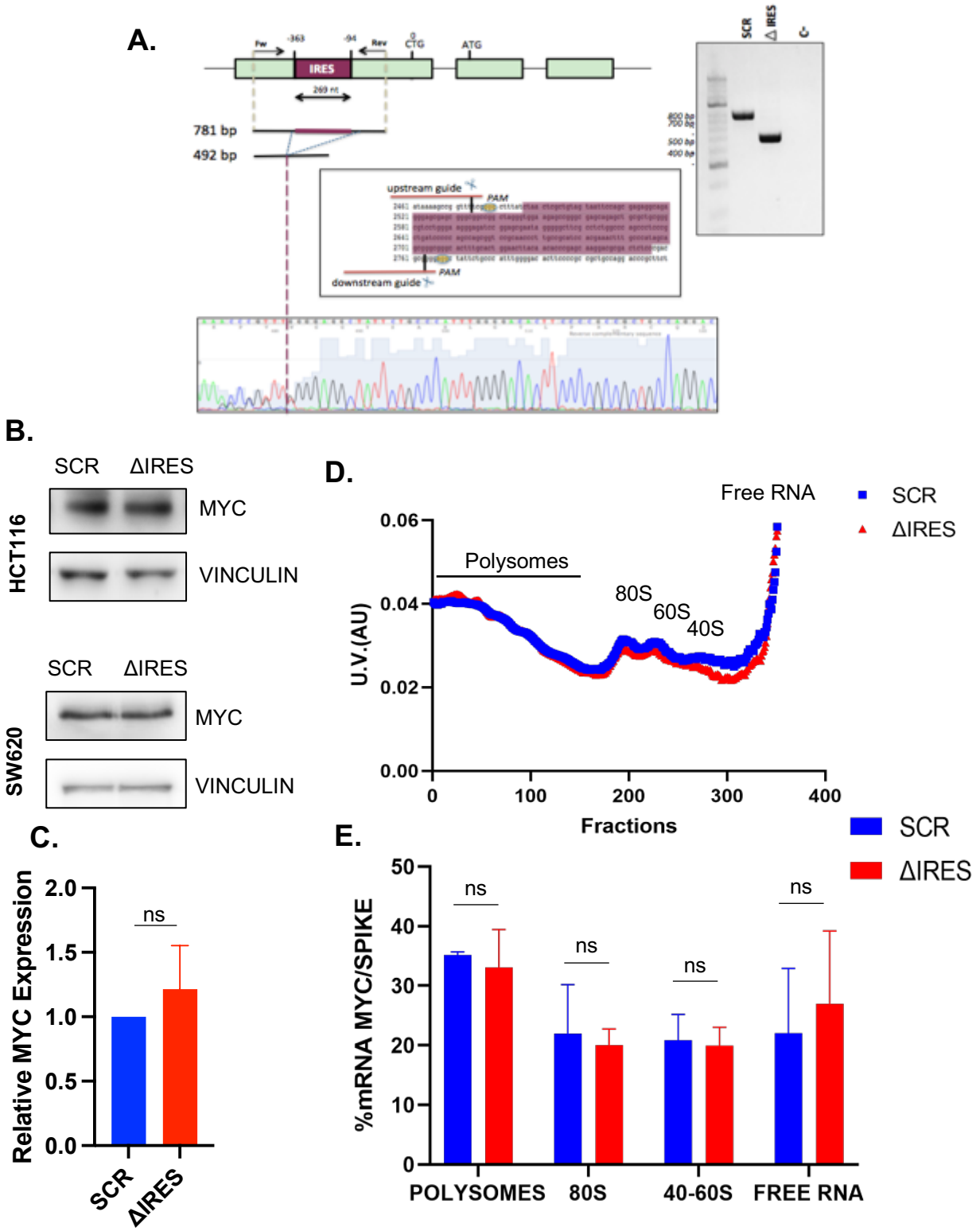

Figure 2. The MYC IRES does not facilitate cap-independent translation in colorectal cancer cells.

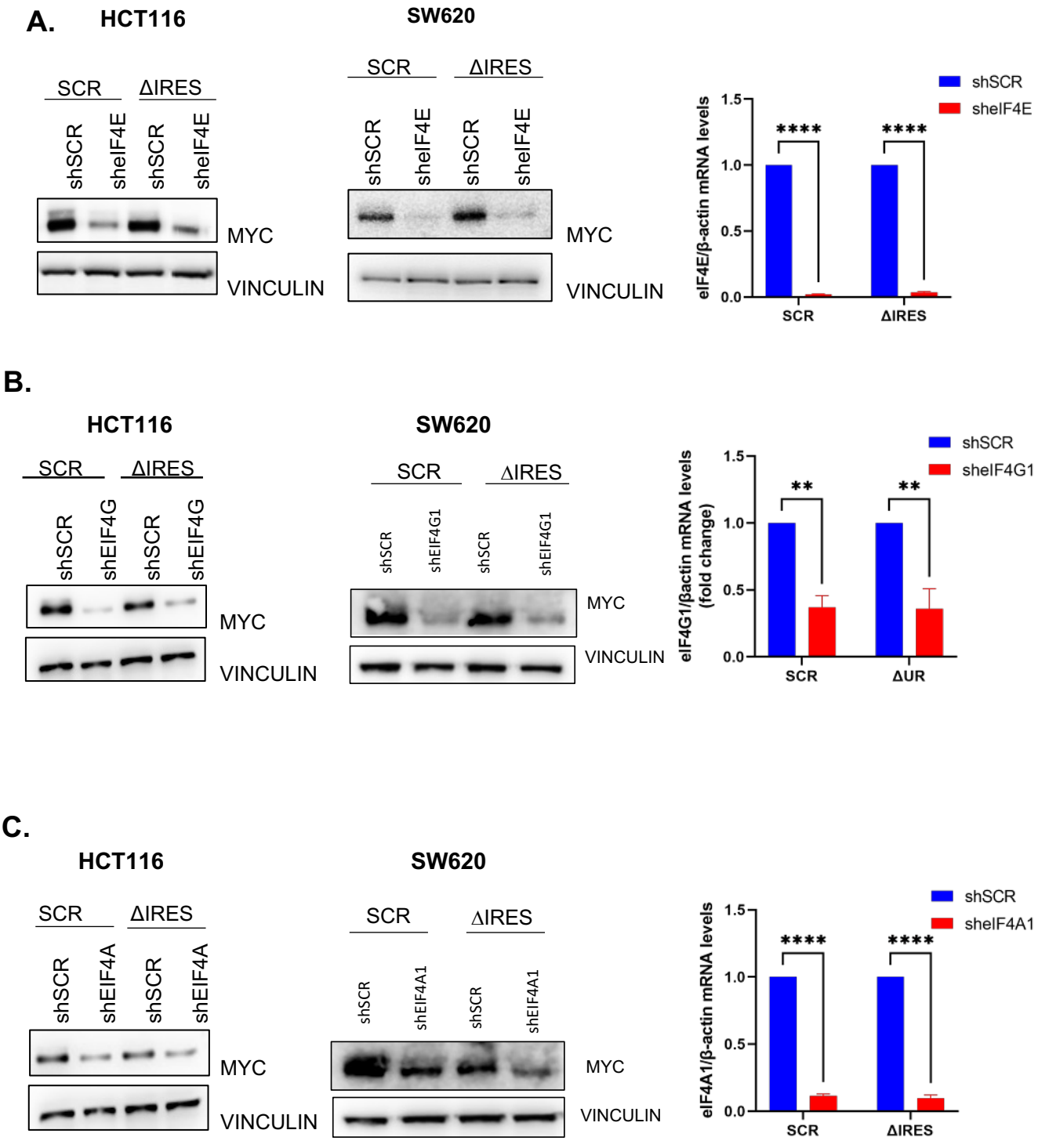

Figure 2 continued. The MYC IRES does not facilitate cap-independent translation in colorectal cancer cells.

D.

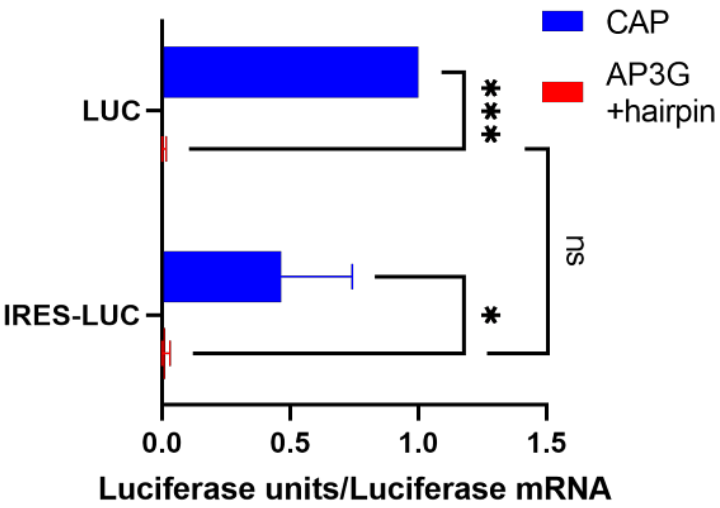

E.

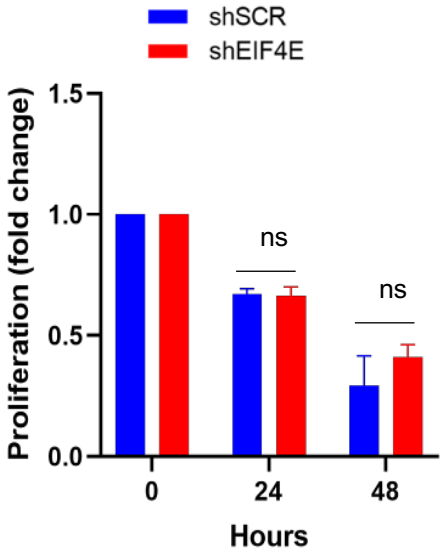

F.

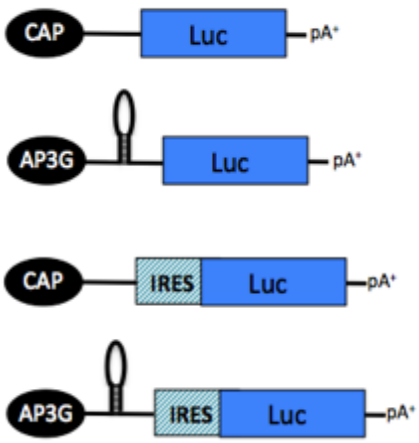

Figure 3. The MYC IRES does not maintain nor facilitate MYC expression during cell stress.

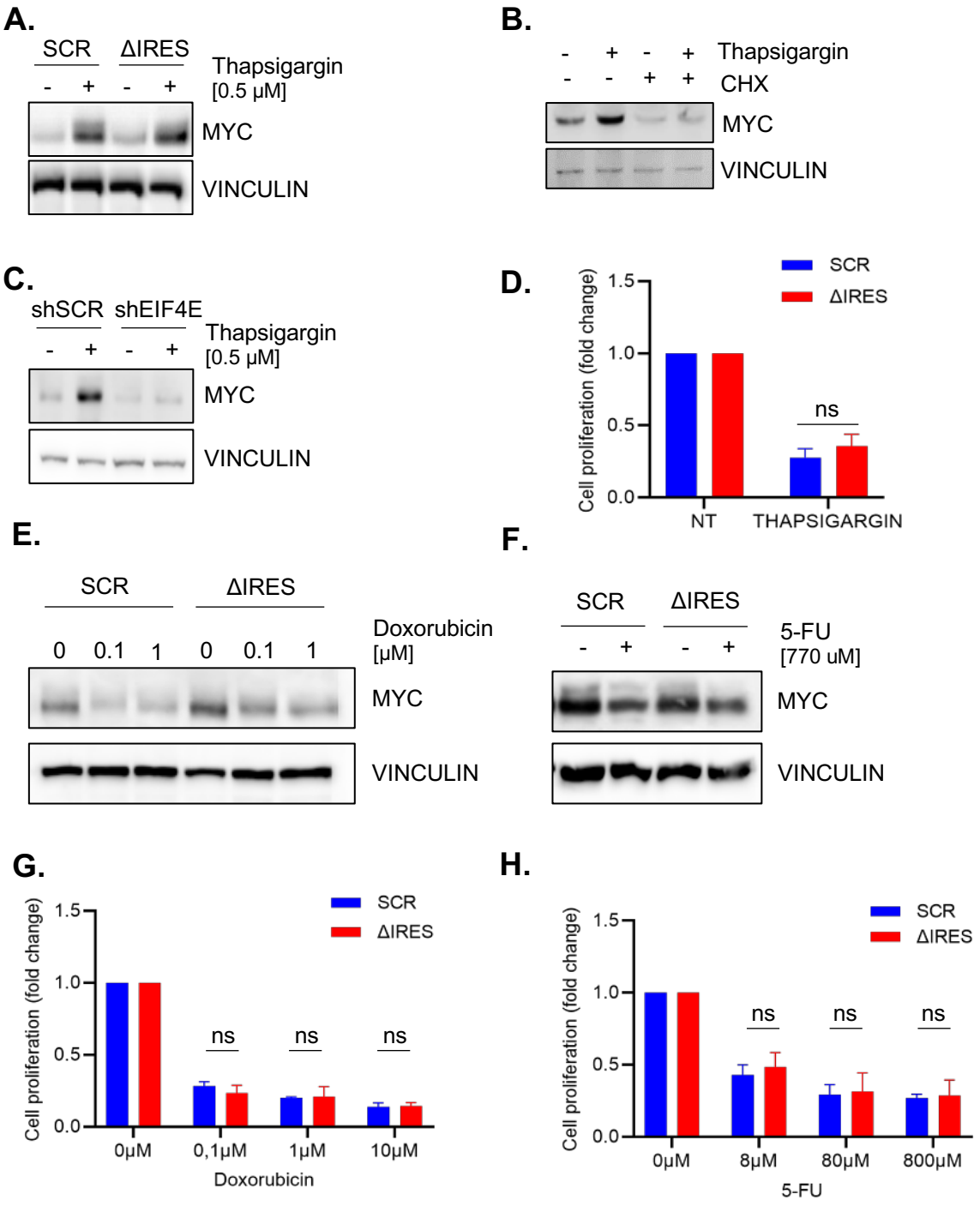

Figure 3 continued. The MYC IRES does not maintain nor facilitate MYC expression during cell stress.

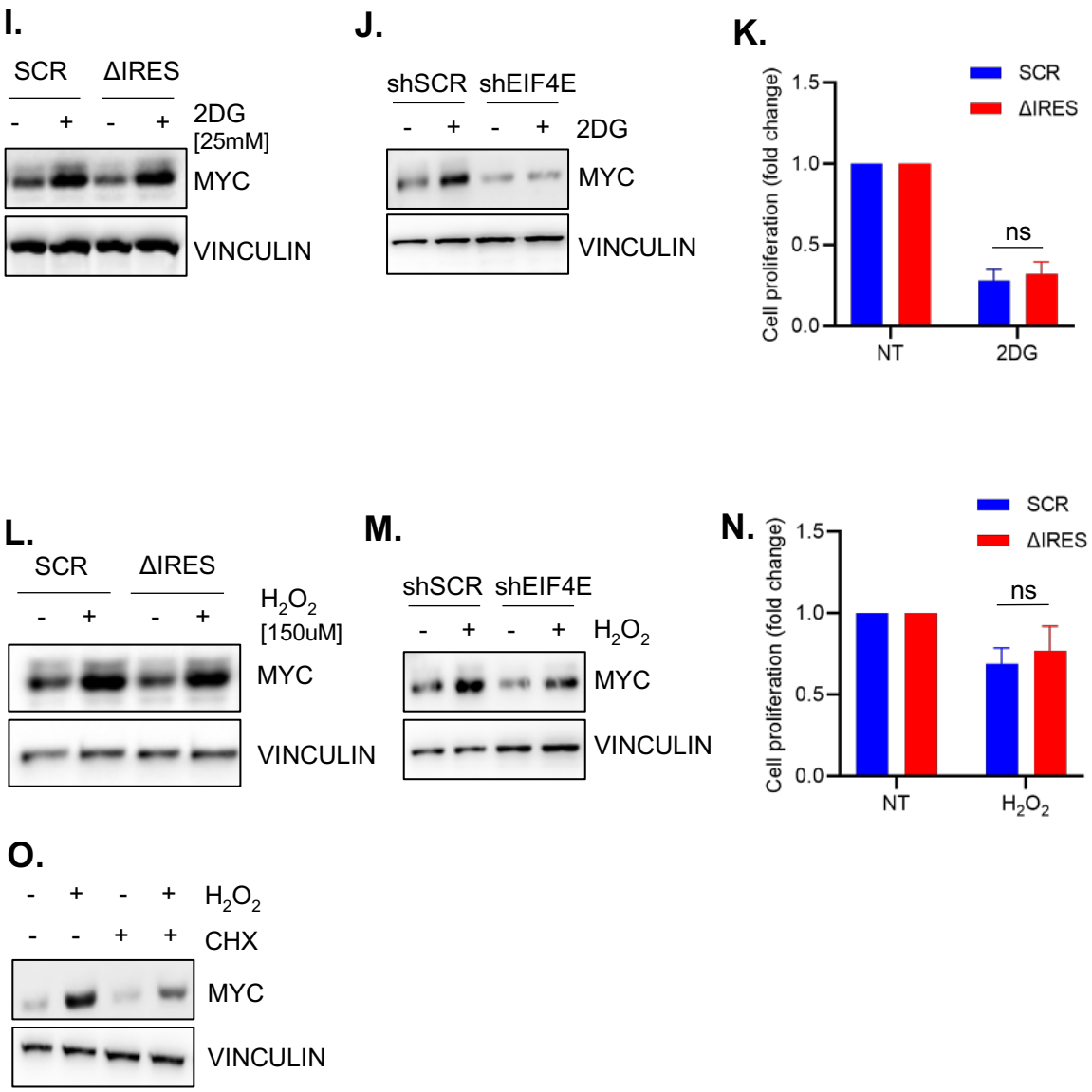

Figure 4. The MYC proximal promoter enhances transcription in response to PI3K inhibition.

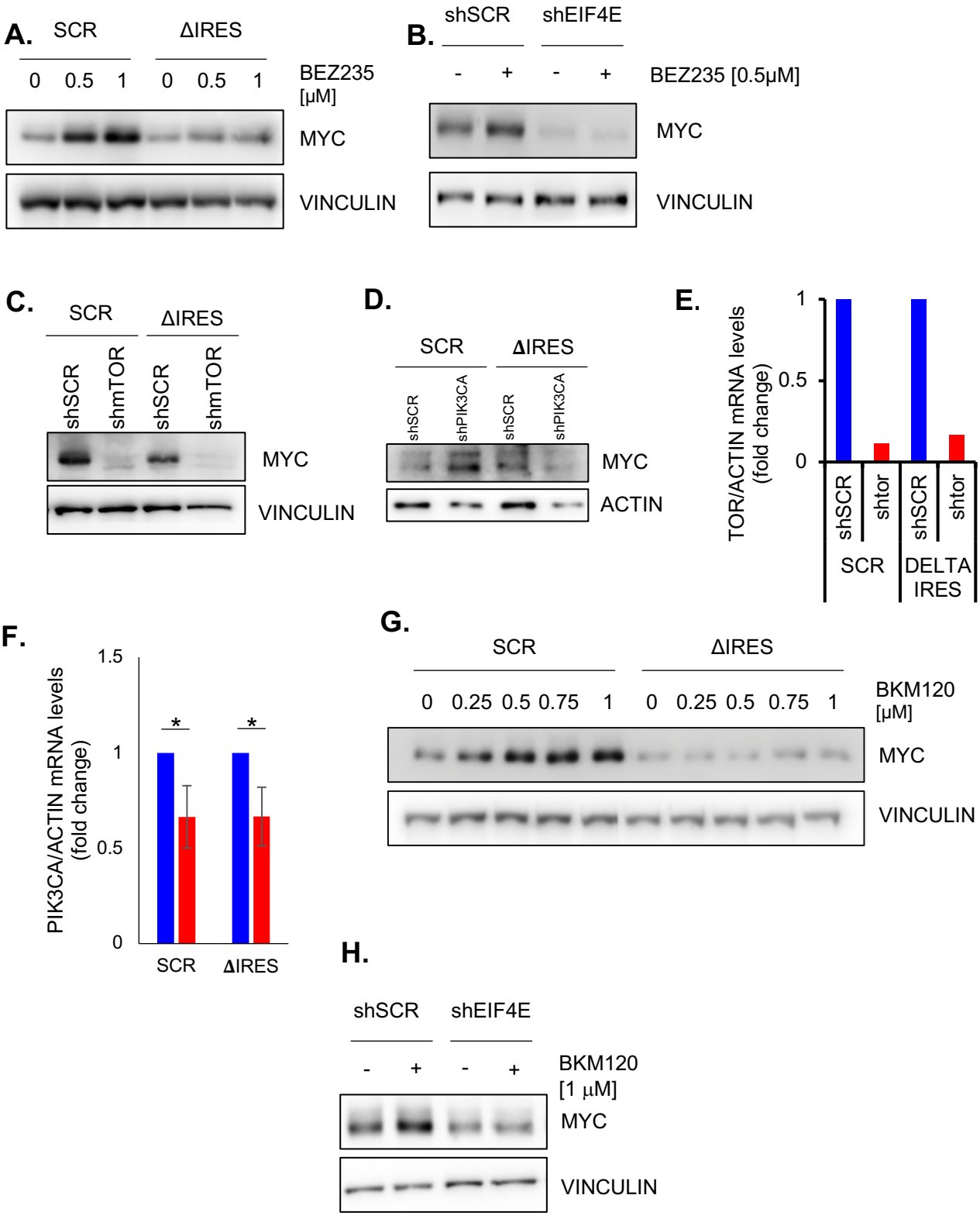

Figure 4 continued. The MYC proximal promoter enhances transcription in response to PI3K inhibition.

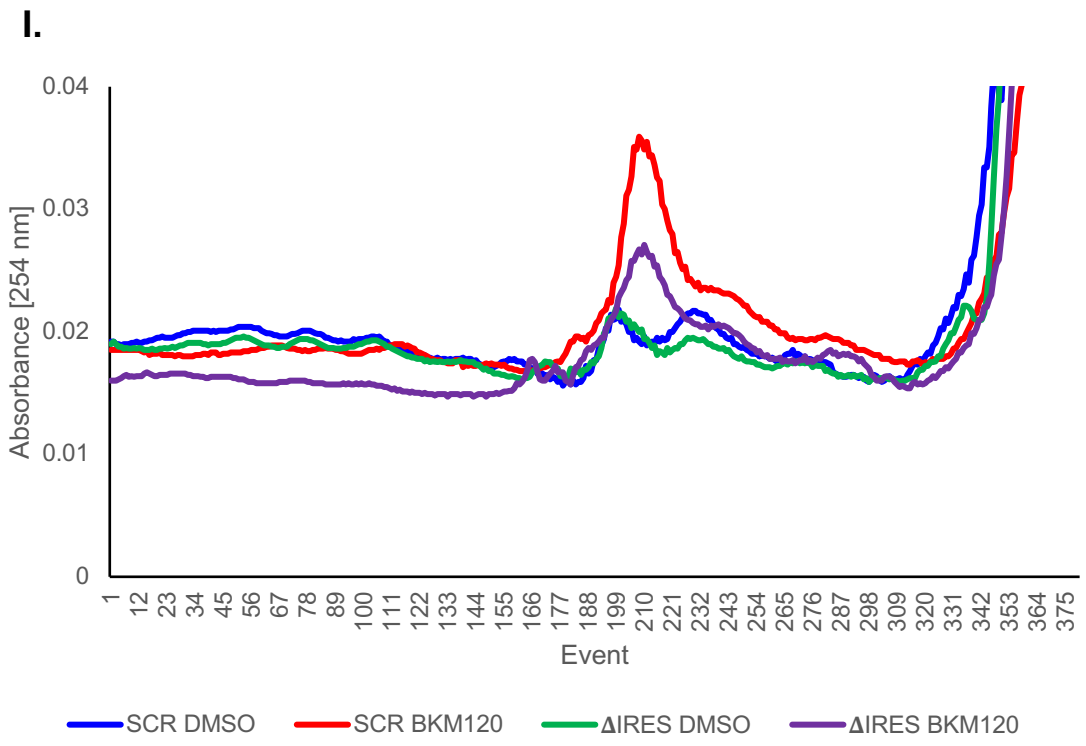

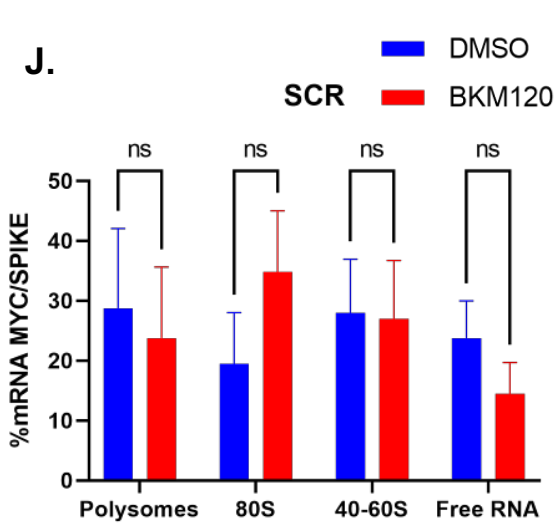

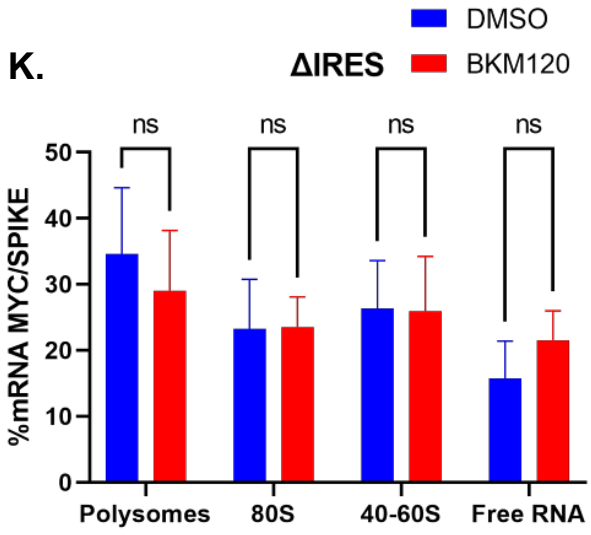

Figure 4 continued. The MYC proximal promoter enhances transcription in response to PI3K inhibition.

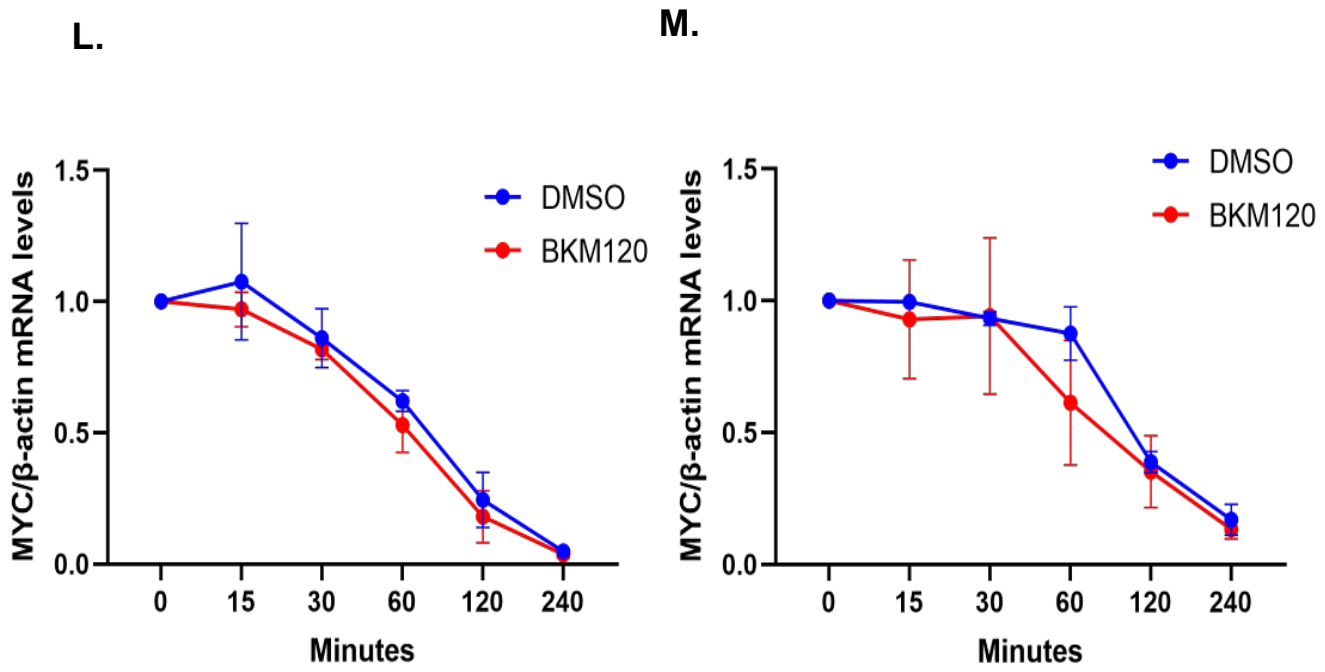

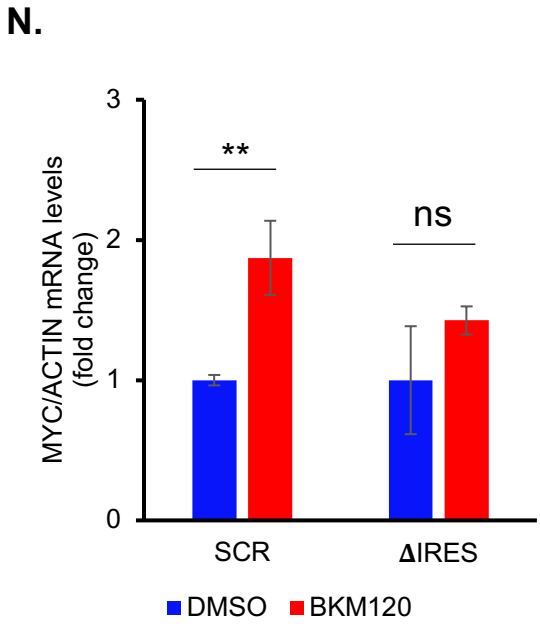

Figure 4 continued. The MYC proximal promoter enhances transcription in response to PI3K inhibition.

O.

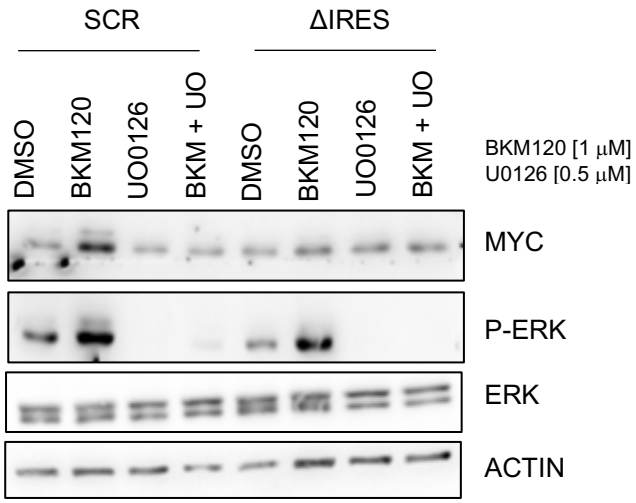

P.

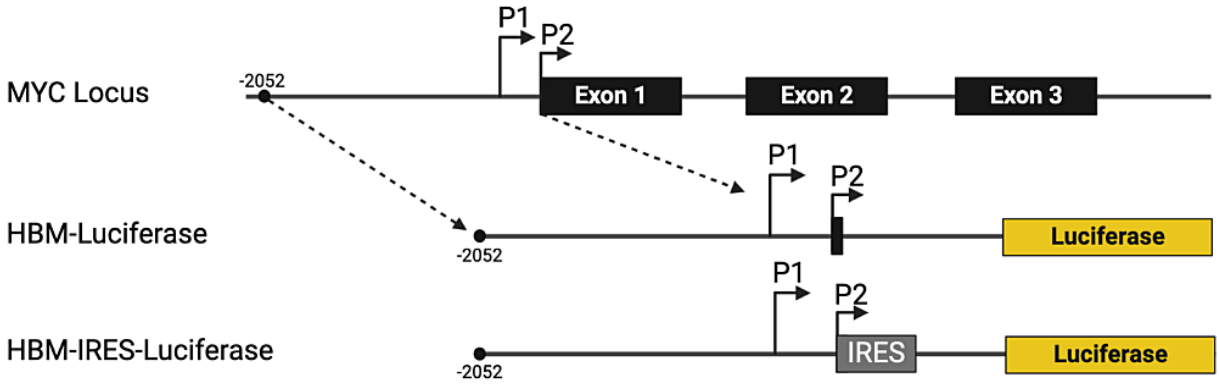

Q.

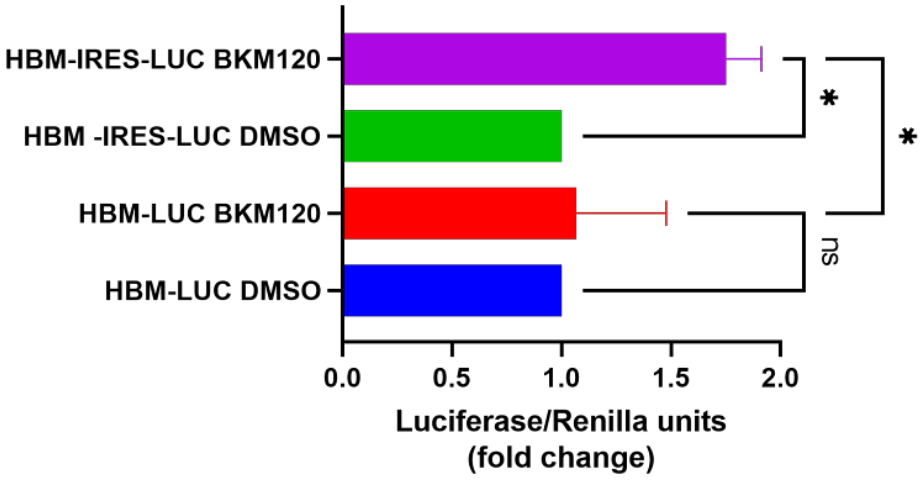

Figure 5. The MYC 5' upstream region provides resistance to PI3K *inhibition in vitro* and *in vivo*.

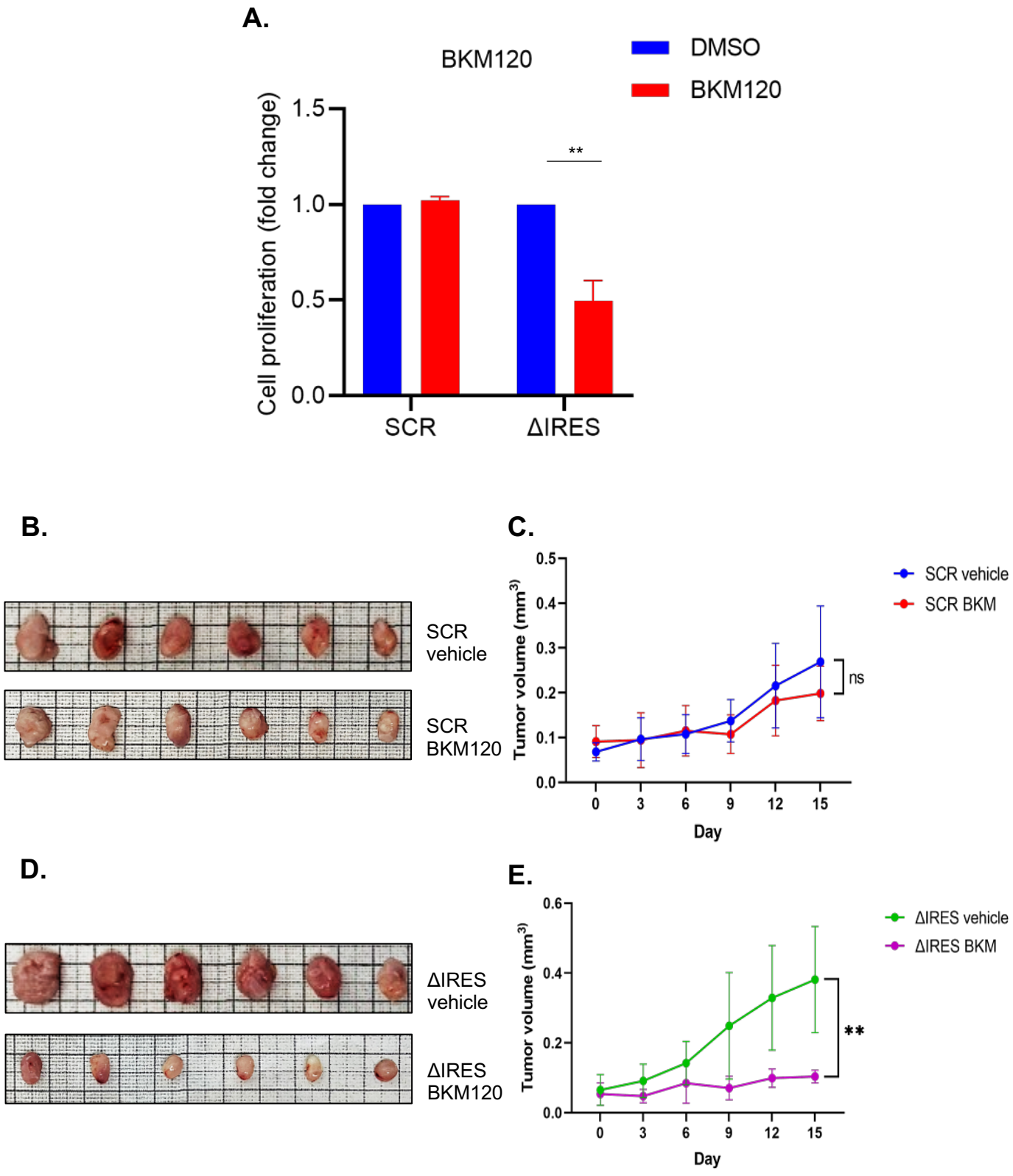

Figure 5 continued. The MYC 5' upstream region provides resistance to PI3K *inhibition in vitro* and *in vivo*.

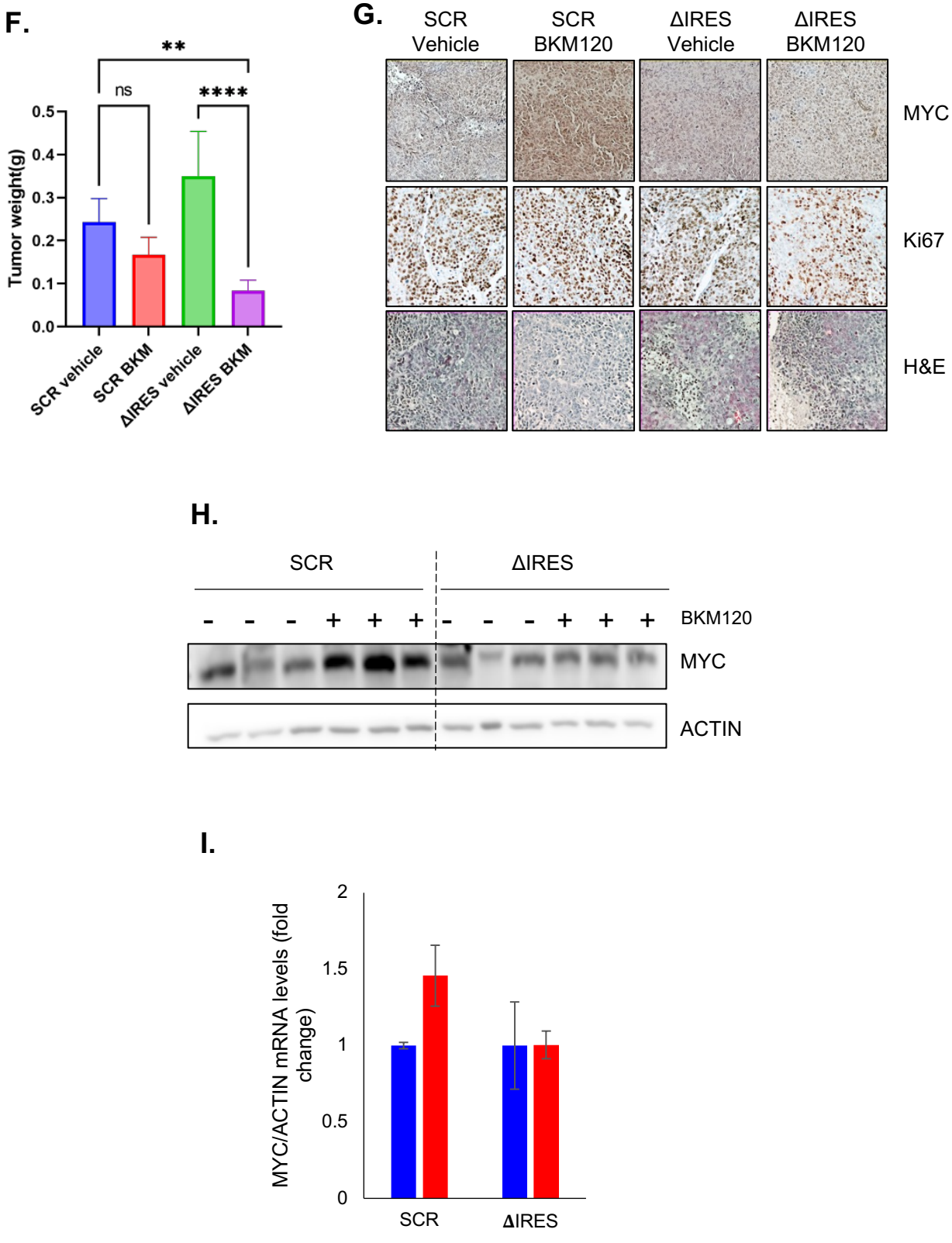

Figure 6. Resistance of colorectal cancer cells to PI3K inhibitors is linked to a MYC-mediated increase of the autophagic flux.

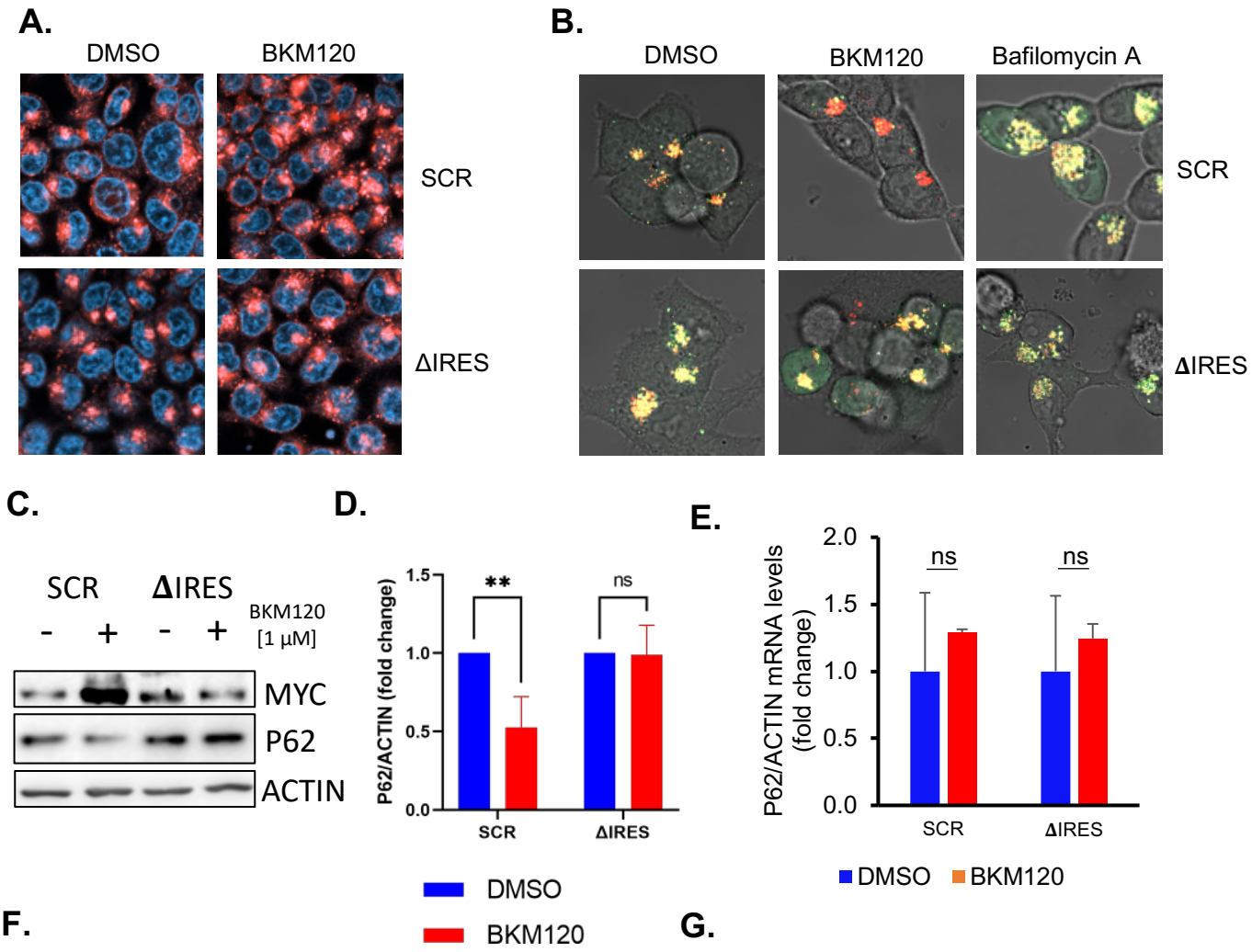

Figure 6 continued. Resistance of colorectal cancer cells to PI3K inhibitors is linked to a MYC-mediated increase of the autophagic flux.

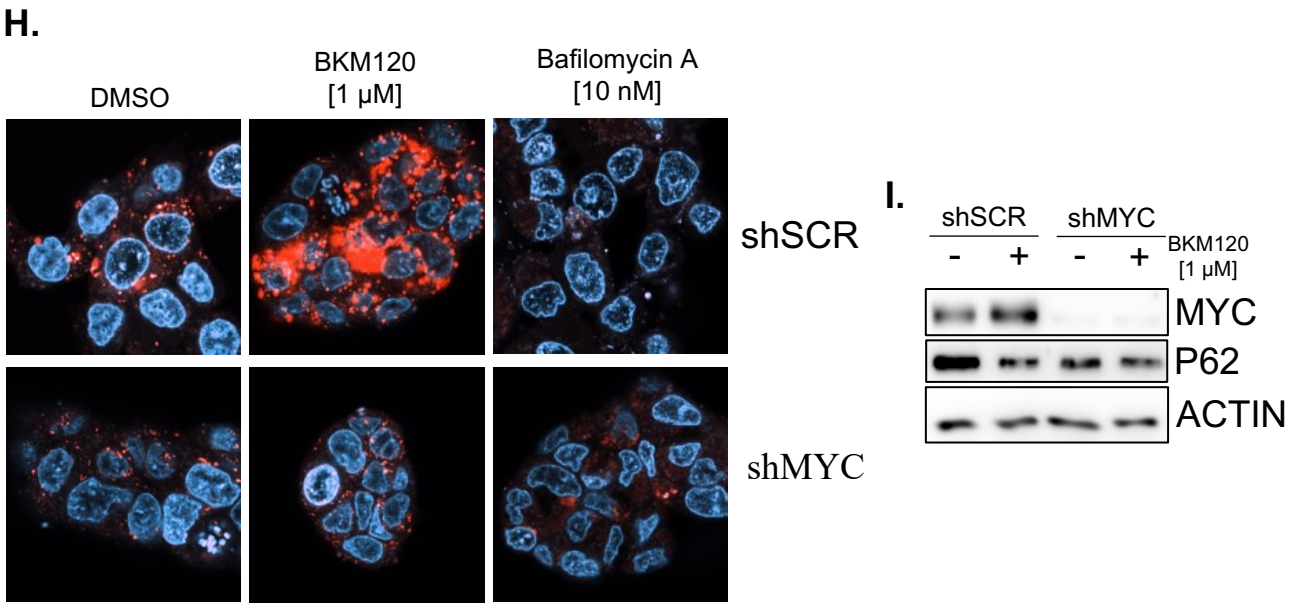

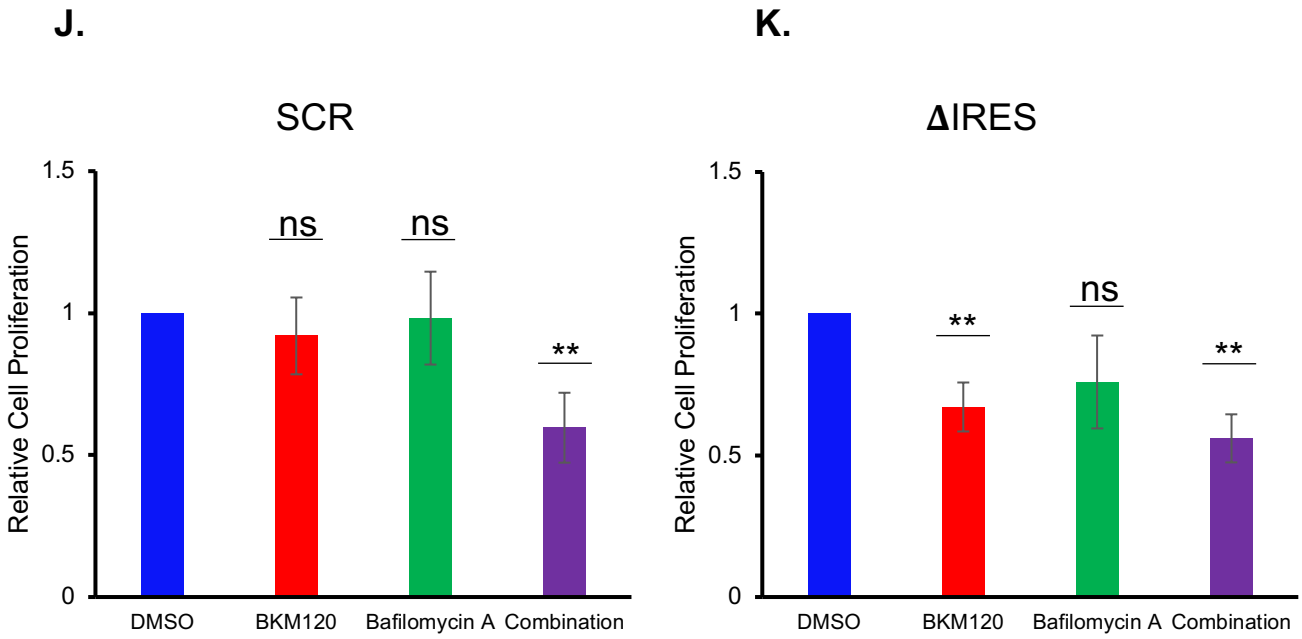

Figure 7. Autophagic resistance to PI3K inhibition mediated by the MYC 5' upstream region is diminished in translocation-specific Burkitt Lymphoma cells.

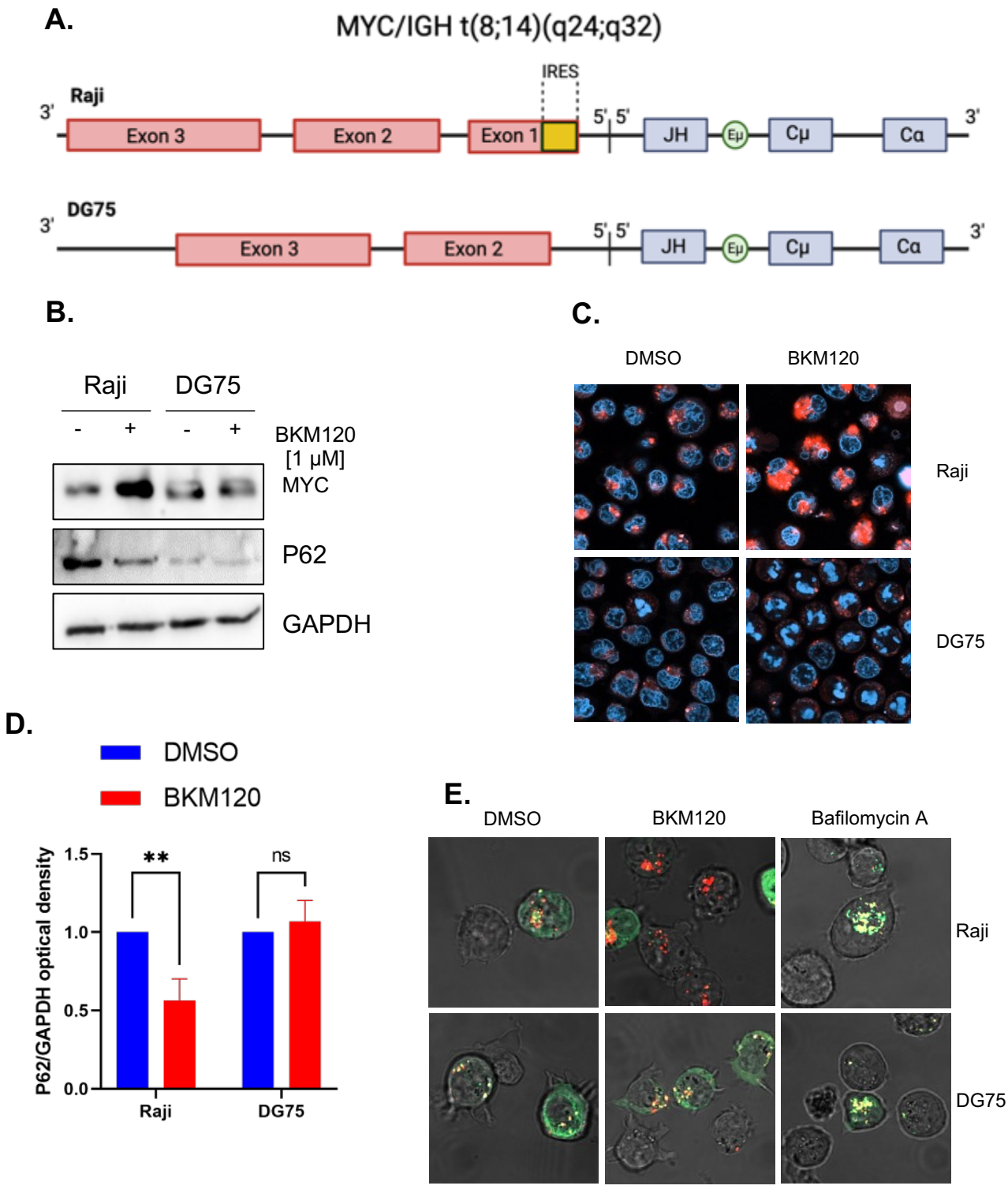

Figure 7 continued. Autophagic resistance to PI3K inhibition mediated by the MYC 5' upstream region is diminished in translocation-specific Burkitt Lymphoma cells.

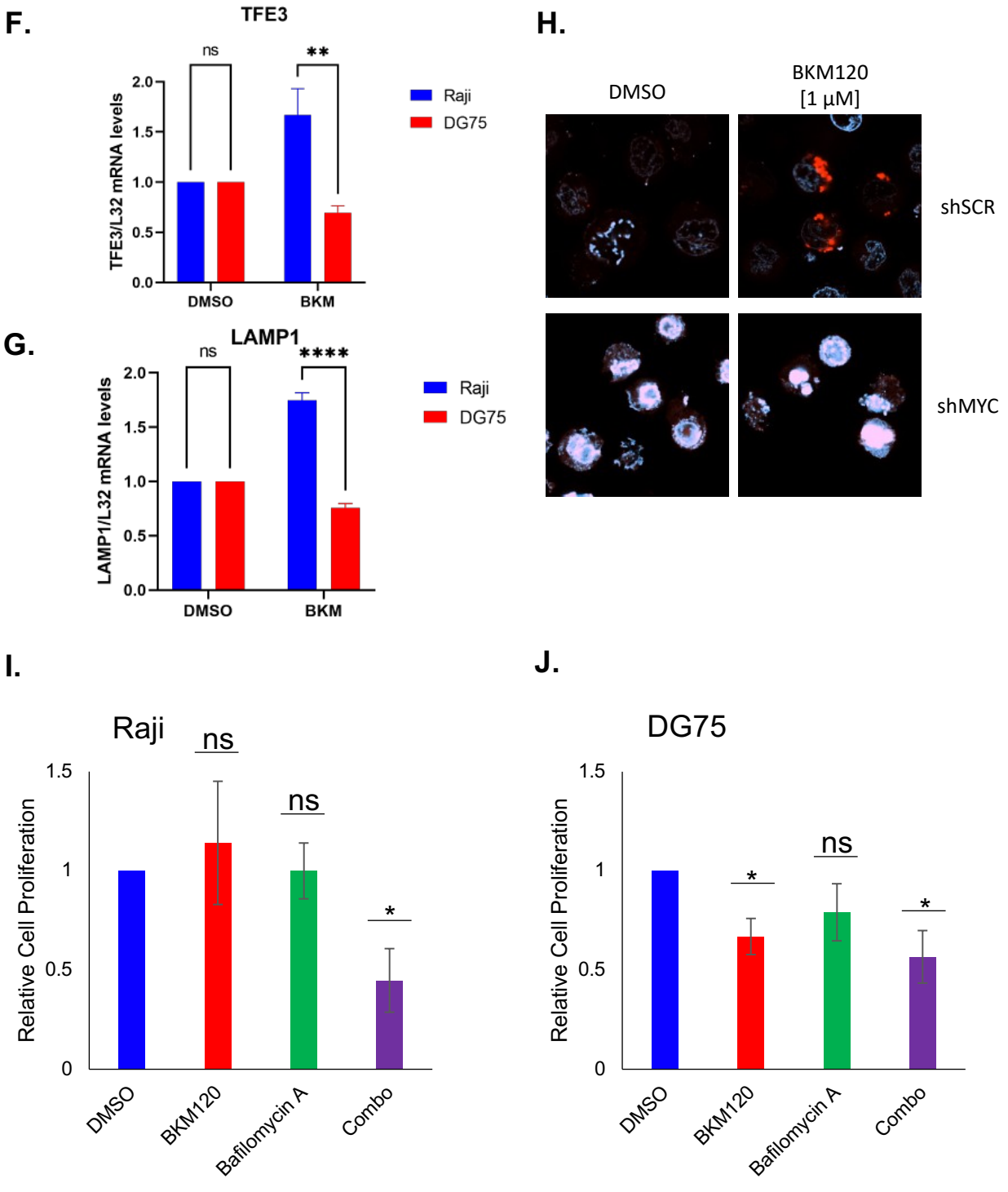

REFERENCES

1. Financial Burden of Cancer Care | Cancer Trends Progress Report. Accessed January 19, 2024. https://progressreport.cancer.gov/after/economic_burden

2. Sung H, Ferlay J, Siegel RL, et al. Global Cancer Statistics 2020: GLOBOCAN Estimates of Incidence and Mortality Worldwide for 36 Cancers in 185 Countries. *CA Cancer J Clin*. 2021;71(3):209-249. doi:10.3322/caac.21660

3. Fearon ER, Vogelstein B. A genetic model for colorectal tumorigenesis. *Cell*. 1990;61(5):759-767. doi:10.1016/0092-8674(90)90186-i

4. Comprehensive molecular characterization of human colon and rectal cancer. *Nature*. 2012;487(7407):330-337. doi:10.1038/nature11252

5. Nguyen LH, Goel A, Chung DC. Pathways of Colorectal Carcinogenesis. *Gastroenterology*. 2020;158(2):291-302. doi:10.1053/j.gastro.2019.08.059

6. Guinney J, Dienstmann R, Wang X, et al. The consensus molecular subtypes of colorectal cancer. *Nat Med*. 2015;21(11):1350-1356. doi:10.1038/nm.3967

7. Research C for DE and. FDA approves pembrolizumab for adults and children with TMB-H solid tumors. *FDA*. Published online June 17, 2020. Accessed December 25, 2023. https://www.fda.gov/drugs/drug-approvals-and-databases/fda-approves-pembrolizumab-adults-and-children-tmb-h-solid-tumors

8. Research C for DE and. FDA grants nivolumab accelerated approval for MSI-H or dMMR colorectal cancer. *FDA*. Published online February 9, 2019. Accessed December 25, 2023. https://www.fda.gov/drugs/resources-information-approved-drugs/fda-grants-nivolumab-accelerated-approval-msi-h-or-dmmr-colorectal-cancer

9. Li K, Luo H, Huang L, Luo H, Zhu X. Microsatellite instability: a review of what the oncologist should know. *Cancer Cell International*. 2020;20(1):16. doi:10.1186/s12935-019-1091-8

10. Hoevenaar WHM, Janssen A, Quirindongo AI, et al. Degree and site of chromosomal instability define its oncogenic potential. *Nat Commun*. 2020;11(1):1501. doi:10.1038/s41467-020-15279-9

11. Dunican DS, McWilliam P, Tighe O, Parle-McDermott A, Croke DT. Gene expression differences between the microsatellite instability (MIN) and chromosomal instability (CIN) phenotypes in colorectal cancer revealed by high-density cDNA array hybridization. *Oncogene*. 2002;21(20):3253-3257. doi:10.1038/sj.onc.1205431

12. Walther A, Houlston R, Tomlinson I. Association between chromosomal instability and prognosis in colorectal cancer: a meta-analysis. *Gut*. 2008;57(7):941-950. doi:10.1136/gut.2007.135004

13. Pino MS, Chung DC. The Chromosomal Instability Pathway in Colon Cancer. *Gastroenterology*. 2010;138(6):2059-2072. doi:10.1053/j.gastro.2009.12.065

14. Rochlitz CF, Herrmann R, de Kant E. Overexpression and amplification of c-myc during progression of human colorectal cancer. *Oncology*. 1996;53(6):448-454. doi:10.1159/000227619

15. Liu J, Xiao Q, Xiao J, et al. Wnt/β-catenin signalling: function, biological mechanisms, and therapeutic opportunities. *Sig Transduct Target Ther*. 2022;7(1):1-23. doi:10.1038/s41392-021-00762-6

16. Haigis KM, Kendall KR, Wang Y, et al. Differential effects of oncogenic K-Ras and N-Ras on proliferation, differentiation and tumor progression in the colon. *Nat Genet*. 2008;40(5):600-608. doi:10.1038/ngXXXX

17. Ros J, Baraibar I, Sardo E, et al. BRAF, MEK and EGFR inhibition as treatment strategies in BRAF V600E metastatic colorectal cancer. *Ther Adv Med Oncol*. 2021;13:1758835921992974. doi:10.1177/1758835921992974

18. Moser AR, Luongo C, Gould KA, McNeley MK, Shoemaker AR, Dove WF. ApcMin: a mouse model for intestinal and mammary tumorigenesis. *Eur J Cancer*. 1995;31A(7-8):1061-1064. doi:10.1016/0959-8049(95)00181-h

19. Sansom OJ, Meniel VS, Muncan V, et al. Myc deletion rescues Apc deficiency in the small intestine. *Nature*. 2007;446(7136):676-679. doi:10.1038/nature05674

20. Eisenman RN. The Max network: coordinated transcriptional regulation of cell growth and proliferation. *Harvey Lect*. 2000;96:1-32.

21. Blackwood EM, Eisenman RN. Max: a helix-loop-helix zipper protein that forms a sequence-specific DNA-binding complex with Myc. *Science*. 1991;251(4998):1211-1217. doi:10.1126/science.2006410

22. Blackwell TK, Kretzner L, Blackwood EM, Eisenman RN, Weintraub H. Sequence-Specific DNA Binding by the c-Myc Protein. *Science*. 1990;250(4984):1149-1151. doi:10.1126/science.2251503

23. Blackwell TK, Huang J, Ma A, et al. Binding of myc proteins to canonical and noncanonical DNA sequences. *Mol Cell Biol*. 1993;13(9):5216-5224. doi:10.1128/mcb.13.9.5216-5224.1993

24. Brenner C, Deplus R, Didelot C, et al. Myc represses transcription through recruitment of DNA methyltransferase corepressor. *EMBO J*. 2005;24(2):336-346. doi:10.1038/sj.emboj.7600509

25. Bouchard C, Dittrich O, Kiermaier A, et al. Regulation of cyclin D2 gene expression by the Myc/Max/Mad network: Myc-dependent TRRAP recruitment and histone acetylation at the cyclin D2 promoter. *Genes Dev*. 2001;15(16):2042-2047. doi:10.1101/gad.907901

26. Cheng SW, Davies KP, Yung E, Beltran RJ, Yu J, Kalpana GV. c-MYC interacts with INI1/hSNF5 and requires the SWI/SNF complex for transactivation function. *Nat Genet*. 1999;22(1):102-105. doi:10.1038/8811

27. Gearhart J, Pashos EE, Prasad MK. Pluripotency Redux — Advances in Stem-Cell Research. *New England Journal of Medicine*. 2007;357(15):1469-1472. doi:10.1056/NEJMp078126

28. Dalla-Favera R, Bregni M, Erikson J, Patterson D, Gallo RC, Croce CM. Human c-myc onc gene is located on the region of chromosome 8 that is translocated in Burkitt lymphoma cells. *Proc Natl Acad Sci U S A*. 1982;79(24):7824-7827. doi:10.1073/pnas.79.24.7824

29. Taub R, Kirsch I, Morton C, et al. Translocation of the c-myc gene into the immunoglobulin heavy chain locus in human Burkitt lymphoma and murine plasmacytoma cells. *Proc Natl Acad Sci U S A*. 1982;79(24):7837-7841. doi:10.1073/pnas.79.24.7837

30. Ray D, Robert-Lézénès J. Coexistence of a c-myc mRNA initiated in intron 1 with the normal c-myc mRNA and similar regulation of both transcripts in mammalian cells. *Oncogene Res*. 1989;5(1):73-78.

31. Bentley DL, Groudine M. Novel promoter upstream of the human c-myc gene and regulation of c-myc expression in B-cell lymphomas. *Mol Cell Biol*. 1986;6(10):3481-3489. doi:10.1128/mcb.6.10.3481-3489.1986

32. Battey J, Moulding C, Taub R, et al. The human c-myc oncogene: structural consequences of translocation into the IgH locus in Burkitt lymphoma. *Cell*. 1983;34(3):779-787. doi:10.1016/0092-8674(83)90534-2

33. Starr DB, Hawley DK. TFIID binds in the minor groove of the TATA box. *Cell*. 1991;67(6):1231-1240. doi:10.1016/0092-8674(91)90299-e

34. Hoopes BC, LeBlanc JF, Hawley DK. Contributions of the TATA box sequence to rate-limiting steps in transcription initiation by RNA polymerase II. *J Mol Biol*. 1998;277(5):1015-1031. doi:10.1006/jmbi.1998.1651

35. Bareket-Samish A, Cohen I, Haran TE. Signals for TBP/TATA box recognition. *J Mol Biol*. 2000;299(4):965-977. doi:10.1006/jmbi.2000.3797

36. Wierstra I, Alves J. The c-myc promoter: still MysterY and challenge. *Adv Cancer Res*. 2008;99:113-333. doi:10.1016/S0065-230X(07)99004-1

37. Chen H, Liu H, Qing G. Targeting oncogenic Myc as a strategy for cancer treatment. *Sig Transduct Target Ther*. 2018;3(1):1-7. doi:10.1038/s41392-018-0008-7

38. Adhikary S, Eilers M. Transcriptional regulation and transformation by Myc proteins. *Nat Rev Mol Cell Biol*. 2005;6(8):635-645. doi:10.1038/nrm1703

39. Meyer N, Penn LZ. Reflecting on 25 years with MYC. *Nat Rev Cancer*. 2008;8(12):976-990. doi:10.1038/nrc2231

40. Dang CV. MYC on the Path to Cancer. *Cell*. 2012;149(1):22-35. doi:10.1016/j.cell.2012.03.003

41. Jung M, Russell AJ, Liu B, et al. A Myc Activity Signature Predicts Poor Clinical Outcomes in Myc-Associated Cancers. *Cancer Res*. 2017;77(4):971-981. doi:10.1158/0008-5472.CAN-15-2906

42. Uhlén M, Fagerberg L, Hallström BM, et al. Tissue-based map of the human proteome. *Science*. 2015;347(6220):1260419. doi:10.1126/science.1260419

43. Tissue expression of MYC - Summary - The Human Protein Atlas. Accessed January 19, 2024. https://www.proteinatlas.org/ENSG00000136997-MYC/tissue#rna_expression

44. Bachmann AS, Geerts D. Polyamine synthesis as a target of MYC oncogenes. *J Biol Chem*. 2018;293(48):18757-18769. doi:10.1074/jbc.TM118.003336

45. Coni S, Bordone R, Ivy DM, et al. Combined inhibition of polyamine metabolism and eIF5A hypusination suppresses colorectal cancer growth through a converging effect on MYC translation. *Cancer Letters*. 2023;559:216120. doi:10.1016/j.canlet.2023.216120

46. Wiegering A, Uthe FW, Jamieson T, et al. Targeting translation initiation bypasses signaling crosstalk mechanisms that maintain high MYC levels in

colorectal cancer. *Cancer Discov*. 2015;5(7):768-781. doi:10.1158/2159-8290.CD-14-1040

47. Wang C, Zhang J, Yin J, et al. Alternative approaches to target Myc for cancer treatment. *Sig Transduct Target Ther*. 2021;6(1):1-14. doi:10.1038/s41392-021-00500-y

48. Llombart V, Mansour MR. Therapeutic targeting of “undruggable” MYC. *EBioMedicine*. 2021;75:103756. doi:10.1016/j.ebiom.2021.103756

49. Hinnebusch AG, Lorsch JR. The Mechanism of Eukaryotic Translation Initiation: New Insights and Challenges. *Cold Spring Harb Perspect Biol*. 2012;4(10):a011544. doi:10.1101/cshperspect.a011544

50. Sonenberg N, Gingras AC. The mRNA 5’ cap-binding protein eIF4E and control of cell growth. *Curr Opin Cell Biol*. 1998;10(2):268-275. doi:10.1016/s0955-0674(98)80150-6

51. Qin X, Jiang B, Zhang Y. 4E-BP1, a multifactor regulated multifunctional protein. *Cell Cycle*. 2016;15(6):781-786. doi:10.1080/15384101.2016.1151581

52. Advani VM, Ivanov P. Translational control under stress: reshaping the translatome. *Bioessays*. 2019;41(5):e1900009. doi:10.1002/bies.201900009

53. Warnakulasuriyarachchi D, Cerquozzi S, Cheung HH, Holcík M. Translational induction of the inhibitor of apoptosis protein HIAP2 during endoplasmic reticulum stress attenuates cell death and is mediated via an

inducible internal ribosome entry site element. *J Biol Chem*. 2004;279(17):17148-17157. doi:10.1074/jbc.M308737200

54. Dobson T, Chen J, Krushel LA. Dysregulating IRES-dependent translation contributes to over-expression of the Aurora A kinase onco-protein. *Mol Cancer Res*. 2013;11(8):887-900. doi:10.1158/1541-7786.MCR-12-0707

55. Blume SW, Jackson NL, Frost AR, et al. Northwestern profiling of potential translation-regulatory proteins in human breast epithelial cells and malignant breast tissues: evidence for pathological activation of the IGF1R IRES. *Exp Mol Pathol*. 2010;88(3):341-352. doi:10.1016/j.yexmp.2010.03.006

56. Blau L, Knirsh R, Ben-Dror I, et al. Aberrant expression of c-Jun in glioblastoma by internal ribosome entry site (IRES)-mediated translational activation. *Proc Natl Acad Sci U S A*. 2012;109(42):E2875-E2884. doi:10.1073/pnas.1203659109

57. Bellodi C, Krasnykh O, Haynes N, et al. Loss of function of the tumor suppressor DKC1 perturbs p27 translation control and contributes to pituitary tumorigenesis. *Cancer Res*. 2010;70(14):6026-6035. doi:10.1158/0008-5472.CAN-09-4730

58. Jang SK, Kräusslich HG, Nicklin MJ, Duke GM, Palmenberg AC, Wimmer E. A segment of the 5’ nontranslated region of encephalomyocarditis

virus RNA directs internal entry of ribosomes during in vitro translation. *J Virol*. 1988;62(8):2636-2643. doi:10.1128/JVI.62.8.2636-2643.1988

59. Pelletier J, Sonenberg N. Internal initiation of translation of eukaryotic mRNA directed by a sequence derived from poliovirus RNA. *Nature*. 1988;334(6180):320-325. doi:10.1038/334320a0

60. Sk J, Hg K, Mj N, Gm D, Ac P, E W. A segment of the 5' nontranslated region of encephalomyocarditis virus RNA directs internal entry of ribosomes during in vitro translation. *Journal of virology*. 1988;62(8). doi:10.1128/JVI.62.8.2636-2643.1988

61. Kieft JS. Viral IRES RNA structures and ribosome interactions. *Trends in Biochemical Sciences*. 2008;33(6):274-283. doi:10.1016/j.tibs.2008.04.007

62. Chen CY, Sarnow P. Initiation of protein synthesis by the eukaryotic translational apparatus on circular RNAs. *Science*. 1995;268(5209):415-417. doi:10.1126/science.7536344

63. Le SY, Maizel JV. A common RNA structural motif involved in the internal initiation of translation of cellular mRNAs. *Nucleic Acids Res*. 1997;25(2):362-369.

64. Jackson RJ, Kaminski A. Internal initiation of translation in eukaryotes: the picornavirus paradigm and beyond. *RNA*. 1995;1(10):985-1000.

65. Fernández IS, Bai XC, Murshudov G, Scheres SHW, Ramakrishnan V. Initiation of Translation by Cricket Paralysis Virus IRES Requires Its

Translocation in the Ribosome. *Cell*. 2014;157(4):823-831. doi:10.1016/j.cell.2014.04.015

66. Lee KM, Chen CJ, Shih SR. Regulation Mechanisms of Viral IRES-Driven Translation. *Trends in Microbiology*. 2017;25(7):546-561. doi:10.1016/j.tim.2017.01.010

67. Yang Y, Wang Z. IRES-mediated cap-independent translation, a path leading to hidden proteome. *Journal of Molecular Cell Biology*. 2019;11(10):911-919. doi:10.1093/jmcb/mjz091

68. Martinez-Salas E, Francisco-Velilla R, Fernandez-Chamorro J, Embarek AM. Insights into Structural and Mechanistic Features of Viral IRES Elements. *Frontiers in Microbiology*. 2018;8. Accessed March 17, 2023. https://www.frontiersin.org/articles/10.3389/fmicb.2017.02629

69. Jan E. Divergent IRES elements in invertebrates. *Virus Res*. 2006;119(1):16-28. doi:10.1016/j.virusres.2005.10.011

70. Kieft JS, Zhou K, Jubin R, Murray MG, Lau JY, Doudna JA. The hepatitis C virus internal ribosome entry site adopts an ion-dependent tertiary fold. *J Mol Biol*. 1999;292(3):513-529. doi:10.1006/jmbi.1999.3095

71. Pettit Kneller EL, Rakotondrafara AM, Miller WA. Cap-independent translation of plant viral RNAs. *Virus Res*. 2006;119(1):63-75. doi:10.1016/j.virusres.2005.10.010

72. Kozak M. A second look at cellular mRNA sequences said to function as internal ribosome entry sites. *Nucleic Acids Res*. 2005;33(20):6593-6602. doi:10.1093/nar/gki958

73. Lemp NA, Hiraoka K, Kasahara N, Logg CR. Cryptic transcripts from a ubiquitous plasmid origin of replication confound tests for cis-regulatory function. *Nucleic Acids Res*. 2012;40(15):7280-7290. doi:10.1093/nar/gks451

74. Wang Z, Weaver M, Magnuson NS. Cryptic promoter activity in the DNA sequence corresponding to the pim-1 5'-UTR. *Nucleic Acids Res*. 2005;33(7):2248-2258. doi:10.1093/nar/gki523

75. Mancuso G, Rugarli EI. A cryptic promoter in the first exon of the SPG4gene directs the synthesis of the 60-kDa spastin isoform. *BMC Biology*. 2008;6(1):31. doi:10.1186/1741-7007-6-31

76. Akirtava C, May GE, McManus CJ. False-positive IRESes from Hoxa9 and other genes resulting from errors in mammalian 5' UTR annotations. *Proc Natl Acad Sci U S A*. 2022;119(36):e2122170119. doi:10.1073/pnas.2122170119

77. Baranick BT, Lemp NA, Nagashima J, Hiraoka K, Kasahara N, Logg CR. Splicing mediates the activity of four putative cellular internal ribosome entry sites. *Proc Natl Acad Sci USA*. 2008;105(12):4733-4738. doi:10.1073/pnas.0710650105

78. Hennecke M, Kwissa M, Metzger K, et al. Composition and arrangement of genes define the strength of IRES-driven translation in bicistronic mRNAs. *Nucleic Acids Res*. 2001;29(16):3327-3334.

79. Fernandez J, Yaman I, Huang C, et al. Ribosome stalling regulates IRES-mediated translation in eukaryotes, a parallel to prokaryotic attenuation. *Mol Cell*. 2005;17(3):405-416. doi:10.1016/j.molcel.2004.12.024

80. Sherrill KW, Byrd MP, Eden MEV, Lloyd RE. BCL-2 Translation Is Mediated via Internal Ribosome Entry during Cell Stress *. *Journal of Biological Chemistry*. 2004;279(28):29066-29074. doi:10.1074/jbc.M402727200

81. Park EH, Lee JM, Blais JD, Bell JC, Pelletier J. Internal translation initiation mediated by the angiogenic factor Tie2. *J Biol Chem*. 2005;280(22):20945-20953. doi:10.1074/jbc.M412744200

82. Stoneley M, Paulin FE, Quesne JPL, Chappell SA, Willis AE. C-Myc 5′ untranslated region contains an internal ribosome entry segment. *Oncogene*. 1998;16(3):423-428. doi:10.1038/sj.onc.1201763

83. Nanbru C, Lafon I, Audigier S, et al. Alternative translation of the proto-oncogene c-myc by an internal ribosome entry site. *J Biol Chem*. 1997;272(51):32061-32066. doi:10.1074/jbc.272.51.32061

84. Stoneley M, Subkhankulova T, Le Quesne JP, et al. Analysis of the c-myc IRES; a potential role for cell-type specific trans-acting factors and the

nuclear compartment. *Nucleic Acids Res*. 2000;28(3):687-694. doi:10.1093/nar/28.3.687

85. Benavides-Serrato A, Saunders JT, Kumar S, et al. m6A-modification of cyclin D1 and c-myc IRESs in glioblastoma controls ITAF activity and resistance to mTOR inhibition. *Cancer Lett*. 2023;562:216178. doi:10.1016/j.canlet.2023.216178

86. Nevins TA, Harder ZM, Korneluk RG, Holcík M. Distinct regulation of internal ribosome entry site-mediated translation following cellular stress is mediated by apoptotic fragments of eIF4G translation initiation factor family members eIF4GI and p97/DAP5/NAT1. *J Biol Chem*. 2003;278(6):3572-3579. doi:10.1074/jbc.M206781200

87. Carter PS, Jarquin-Pardo M, De Benedetti A. Differential expression of Myc1 and Myc2 isoforms in cells transformed by eIF4E: evidence for internal ribosome repositioning in the human c-myc 5'UTR. *Oncogene*. 1999;18(30):4326-4335. doi:10.1038/sj.onc.1202890

88. Kim J, Aftab BT, Tang JY, et al. Itraconazole and arsenic trioxide inhibit hedgehog pathway activation and tumor growth associated with acquired resistance to smoothened antagonists. *Cancer cell*. 2013;23(1):23. doi:10.1016/j.ccr.2012.11.017

89. Dyer BW, Ferrer FA, Klinedinst DK, Rodriguez R. A noncommercial dual luciferase enzyme assay system for reporter gene analysis. *Anal Biochem*. 2000;282(1):158-161. doi:10.1006/abio.2000.4605

90. Coni S, Serrao SM, Yurtsever ZN, et al. Blockade of EIF5A hypusination limits colorectal cancer growth by inhibiting MYC elongation. *Cell Death Dis*. 2020;11(12):1-14. doi:10.1038/s41419-020-03174-6

91. D'Amico D, Antonucci L, Di Magno L, et al. Non-canonical Hedgehog/AMPK-Mediated Control of Polyamine Metabolism Supports Neuronal and Medulloblastoma Cell Growth. *Developmental Cell*. 2015;35(1):21-35. doi:10.1016/j.devcel.2015.09.008

92. Graham FL, van der Eb AJ. A new technique for the assay of infectivity of human adenovirus 5 DNA. *Virology*. 1973;52(2):456-467. doi:10.1016/0042-6822(73)90341-3

93. Jinek M, East A, Cheng A, Lin S, Ma E, Doudna J. RNA-programmed genome editing in human cells. Weigel D, ed. *eLife*. 2013;2:e00471. doi:10.7554/eLife.00471

94. Rogers GW, Komar AA, Merrick WC. eIF4A: The godfather of the DEAD box helicases. In: *Progress in Nucleic Acid Research and Molecular Biology*. Vol 72. Academic Press; 2002:307-331. doi:10.1016/S0079-6603(02)72073-4

95. Spriggs KA, Cobbold LC, Jopling CL, et al. Canonical Initiation Factor Requirements of the Myc Family of Internal Ribosome Entry Segments. *Mol Cell Biol*. 2009;29(6):1565-1574. doi:10.1128/MCB.01283-08

96. Prévôt D, Darlix JL, Ohlmann T. Conducting the initiation of protein synthesis: the role of eIF4G. *Biol Cell*. 2003;95(3-4):141-156. doi:10.1016/s0248-4900(03)00031-5

97. Muttach F, Muthmann N, Rentmeister A. Synthetic mRNA capping. *Beilstein J Org Chem*. 2017;13:2819-2832. doi:10.3762/bjoc.13.274

98. Shi Y, Yang Y, Hoang B, et al. Therapeutic potential of targeting IRES-dependent c-myc translation in multiple myeloma cells during ER stress. *Oncogene*. 2016;35(8):1015-1024. doi:10.1038/onc.2015.156

99. Shi Y, Sun F, Cheng Y, et al. Critical Role for Cap-Independent c-MYC Translation in Progression of Multiple Myeloma. *Molecular Cancer Therapeutics*. 2022;21(4):502-510. doi:10.1158/1535-7163.MCT-21-0016

100. Subkhankulova T, Mitchell SA, Willis AE. Internal ribosome entry segment-mediated initiation of c-Myc protein synthesis following genotoxic stress. *Biochem J*. 2001;359(Pt 1):183-192.

101. Pommier Y, Leo E, Zhang H, Marchand C. DNA Topoisomerases and Their Poisoning by Anticancer and Antibacterial Drugs. *Chemistry & Biology*. 2010;17(5):421-433. doi:10.1016/j.chembiol.2010.04.012

102. Huehls AM, Huntoon CJ, Joshi PM, et al. Genomically Incorporated 5-Fluorouracil that Escapes UNG-Initiated Base Excision Repair Blocks DNA Replication and Activates Homologous Recombination. *Mol Pharmacol*. 2016;89(1):53-62. doi:10.1124/mol.115.100164

103. Yeh DW, Zhao X, Siddique HR, et al. MSI2 promotes translation of multiple IRES-containing oncogenes and virus to induce self-renewal of tumor initiating stem-like cells. *Cell Death Discov*. 2023;9(1):1-15. doi:10.1038/s41420-023-01427-9

104. Brown J. Effects of 2-deoxyglucose on carbohydrate metablism: review of the literature and studies in the rat. *Metabolism*. 1962;11:1098-1112.

105. Raman D, Pervaiz S. P-32 - The tumor environment stabilizes c-Myc oncoprotein through its sustained phosphorylation at serine 62, which promotes its oncogenic activity. *Free Radical Biology and Medicine*. 2018;120:S54. doi:10.1016/j.freeradbiomed.2018.04.179

106. Katso R, Okkenhaug K, Ahmadi K, White S, Timms J, Waterfield MD. Cellular Function of Phosphoinositide 3-Kinases: Implications for Development, Immunity, Homeostasis, and Cancer. *Annual Review of Cell and Developmental Biology*. 2001;17(1):615-675. doi:10.1146/annurev.cellbio.17.1.615

107. Sasaki T, Irie-Sasaki J, Horie Y, et al. Colorectal carcinomas in mice lacking the catalytic subunit of PI(3)Kγ. *Nature*. 2000;406(6798):897-902. doi:10.1038/35022585

108. Danielsen SA, Eide PW, Nesbakken A, Guren T, Leithe E, Lothe RA. Portrait of the PI3K/AKT pathway in colorectal cancer. *Biochimica et Biophysica Acta (BBA) - Reviews on Cancer*. 2015;1855(1):104-121. doi:10.1016/j.bbcan.2014.09.008

109. Voutsadakis IA. The Landscape of PIK3CA Mutations in Colorectal Cancer. *Clinical Colorectal Cancer*. 2021;20(3):201-215. doi:10.1016/j.clcc.2021.02.003

110. Zhu J, Blenis J, Yuan J. Activation of PI3K/Akt and MAPK pathways regulates Myc-mediated transcription by phosphorylating and promoting the degradation of Mad1. *Proc Natl Acad Sci U S A*. 2008;105(18):6584-6589. doi:10.1073/pnas.0802785105

111. Singleton KR, Crawford L, Tsui E, et al. Melanoma Therapeutic Strategies that Select against Resistance by Exploiting MYC-Driven Evolutionary Convergence. *Cell Reports*. 2017;21(10):2796-2812. doi:10.1016/j.celrep.2017.11.022

112. Strippoli A, Cocomazzi A, Basso M, et al. c-MYC Expression Is a Possible Keystone in the Colorectal Cancer Resistance to EGFR Inhibitors. *Cancers (Basel)*. 2020;12(3):638. doi:10.3390/cancers12030638

113. Kugimiya N, Nishimoto A, Hosoyama T, et al. The c-MYC-ABCB5 axis plays a pivotal role in 5-fluorouracil resistance in human colon cancer cells. *J Cell Mol Med*. 2015;19(7):1569-1581. doi:10.1111/jcmm.12531

114. Burger MT, Pecchi S, Wagman A, et al. Identification of NVP-BKM120 as a Potent, Selective, Orally Bioavailable Class I PI3 Kinase Inhibitor for Treating Cancer. *ACS Med Chem Lett*. 2011;2(10):774-779. doi:10.1021/ml200156t

115. Bordeleau ME, Robert F, Gerard B, et al. Therapeutic suppression of translation initiation modulates chemosensitivity in a mouse lymphoma model. *J Clin Invest*. 2008;118(7):2651-2660. doi:10.1172/JCI34753

116. DeSilva DR, Jones EA, Favata MF, et al. Inhibition of mitogen-activated protein kinase kinase blocks T cell proliferation but does not induce or prevent anergy. *J Immunol*. 1998;160(9):4175-4181.

117. Duncia JV, Santella JB, Higley CA, et al. MEK inhibitors: The chemistry and biological activity of U0126, its analogs, and cyclization products. *Bioorganic & Medicinal Chemistry Letters*. 1998;8(20):2839-2844. doi:10.1016/S0960-894X(98)00522-8

118. Facchini LM, Chen S, Marhin WW, Lear JN, Penn LZ. The Myc negative autoregulation mechanism requires Myc-Max association and involves the c-myc P2 minimal promoter. *Mol Cell Biol*. 1997;17(1):100-114. doi:10.1128/MCB.17.1.100

119. Polivka J, Janku F. Molecular targets for cancer therapy in the PI3K/AKT/mTOR pathway. *Pharmacol Ther*. 2014;142(2):164-175. doi:10.1016/j.pharmthera.2013.12.004

120. Mishra R, Patel H, Alanazi S, Kilroy MK, Garrett JT. PI3K Inhibitors in Cancer: Clinical Implications and Adverse Effects. *Int J Mol Sci*. 2021;22(7):3464. doi:10.3390/ijms22073464

121. Wright SCE, Vasilevski N, Serra V, Rodon J, Eichhorn PJA. Mechanisms of Resistance to PI3K Inhibitors in Cancer: Adaptive Responses, Drug Tolerance and Cellular Plasticity. *Cancers*. 2021;13(7):1538. doi:10.3390/cancers13071538

122. *Acute Oral Toxicity of DMSO (Dimethyl Sulfoxide) Process Stream Samples in Male and Female Mice.* Accessed January 7, 2024. https://apps.dtic.mil/sti/citations/ADA137228

123. Bhin J, Yemelyanenko J, Chao X, et al. MYC is a clinically significant driver of mTOR inhibitor resistance in breast cancer. *J Exp Med*. 2023;220(11):e20211743. doi:10.1084/jem.20211743

124. Donati G, Amati B. MYC and therapy resistance in cancer: risks and opportunities. *Mol Oncol*. 2022;16(21):3828-3854. doi:10.1002/1878-0261.13319

125. Ren H, Guo H, Thakur A, et al. Blockade efficacy of MEK/ERK-dependent autophagy enhances PI3K/Akt inhibitor NVP-BKM120's

therapeutic effectiveness in lung cancer cells. *Oncotarget*. 2016;7(41):67277-67287. doi:10.18632/oncotarget.11645

126. Toh PPC, Luo S, Menzies FM, Raskó T, Wanker EE, Rubinsztein DC. Myc inhibition impairs autophagosome formation. *Human Molecular Genetics*. 2013;22(25):5237-5248. doi:10.1093/hmg/ddt381

127. Pankiv S, Clausen TH, Lamark T, et al. p62/SQSTM1 Binds Directly to Atg8/LC3 to Facilitate Degradation of Ubiquitinated Protein Aggregates by Autophagy *. *Journal of Biological Chemistry*. 2007;282(33):24131-24145. doi:10.1074/jbc.M702824200

128. Tanida I, Ueno T, Kominami E. LC3 and Autophagy. In: Deretic V, ed. *Autophagosome and Phagosome*. Methods in Molecular Biology™. Humana Press; 2008:77-88. doi:10.1007/978-1-59745-157-4_4

129. Bjørkøy G, Lamark T, Pankiv S, Øvervatn A, Brech A, Johansen T. Monitoring autophagic degradation of p62/SQSTM1. *Methods Enzymol*. 2009;452:181-197. doi:10.1016/S0076-6879(08)03612-4

130. Roschewski M, Staudt LM, Wilson WH. Burkitt's Lymphoma. *New England Journal of Medicine*. 2022;387(12):1111-1122. doi:10.1056/NEJMra2025746

131. Smardova J, Grochova D, Fabian P, et al. An unusual p53 mutation detected in Burkitt's lymphoma: 30 bp duplication. *Oncology Reports*. 2008;20(4):773-778. doi:10.3892/or_00000073

132. Expression of normal and translocated c-myc alleles in Burkitt's lymphoma cells: evidence for different regulation. Accessed January 3, 2024. https://www.embopress.org/doi/epdf/10.1002/j.1460-2075.1989.tb03602.x

133. Nishikura K, Erikson J, ar-Rushdi A, Huebner K, Croce CM. The translocated c-myc oncogene of Raji Burkitt lymphoma cells is not expressed in human lymphoblastoid cells. *Proceedings of the National Academy of Sciences of the United States of America*. 1985;82(9):2900. doi:10.1073/pnas.82.9.2900

134. Molyneux EM, Rochford R, Griffin B, et al. Burkitt's lymphoma. *The Lancet*. 2012;379(9822):1234-1244. doi:10.1016/S0140-6736(11)61177-X

135. Magrath I. The Pathogenesis of Burkitt's Lymphoma. In: Vande Woude GF, Klein G, eds. *Advances in Cancer Research*. Vol 55. Academic Press; 1990:133-270. doi:10.1016/S0065-230X(08)60470-4

136. Barriga F, Kiwanuka J, Alvarez-Mon M, et al. Significance of Chromosome 8 Breakpoint Location in Burkitt's Lymphoma: Correlation with Geographical Origin and Association with Epstein-Barr Virus. In: Potter M, Melchers F, eds. *Mechanisms in B-Cell Neoplasia 1988*. Current Topics in Microbiology and Immunology. Springer; 1988:128-137. doi:10.1007/978-3-642-74006-0_18

137. López C, Kleinheinz K, Aukema SM, et al. Genomic and transcriptomic changes complement each other in the pathogenesis of sporadic Burkitt lymphoma. *Nat Commun*. 2019;10(1):1459. doi:10.1038/s41467-019-08578-3

138. Busch K, Keller T, Fuchs U, et al. Identification of two distinct MYC breakpoint clusters and their association with various IGH breakpoint regions in the t(8;14) translocations in sporadic Burkitt-lymphoma. *Leukemia*. 2007;21(8):1739-1751. doi:10.1038/sj.leu.2404753

139. Bellan C, Lazzi S, Falco GD, Nyongo A, Giordano A, Leoncini L. Burkitt's lymphoma: new insights into molecular pathogenesis. *Journal of Clinical Pathology*. 2003;56(3):188. doi:10.1136/jcp.56.3.188

140. Shiramizu B, Magrath I. Localization of breakpoints by polymerase chain reactions in Burkitt's lymphoma with 8;14 translocations. *Blood*. 1990;75(9):1848-1852.

141. Basso K, Frascella E, Zanesco L, Rosolen A. Improved Long-Distance Polymerase Chain Reaction for the Detection of t(8;14)(q24;q32) in Burkitt's Lymphomas. *Am J Pathol*. 1999;155(5):1479-1485.

142. Bretones G, Delgado MD, León J. Myc and cell cycle control. *Biochim Biophys Acta*. 2015;1849(5):506-516. doi:10.1016/j.bbagrm.2014.03.013

143. D'Amico D, Antonucci L, Di Magno L, et al. Non-canonical Hedgehog/AMPK-Mediated Control of Polyamine Metabolism Supports

Neuronal and Medulloblastoma Cell Growth. *Developmental Cell*. 2015;35(1):21-35. doi:10.1016/j.devcel.2015.09.008

144. Yang J, Nie J, Ma X, Wei Y, Peng Y, Wei X. Targeting PI3K in cancer: mechanisms and advances in clinical trials. *Molecular Cancer*. 2019;18(1):26. doi:10.1186/s12943-019-0954-x

145. Press Announcements - FDA approves Zydelig for three types of blood cancers. Accessed January 20, 2024. https://wayback.archive-it.org/7993/20170112023830/http://www.fda.gov/NewsEvents/Newsroom/PressAnnouncements/ucm406387.htm

146. FDA approves new treatment for adults with relapsed follicular lymphoma | FDA. Accessed January 20, 2024. https://www.fda.gov/news-events/press-announcements/fda-approves-new-treatment-adults-relapsed-follicular-lymphoma

147. Commissioner O of the. FDA approves first PI3K inhibitor for breast cancer. FDA. Published March 24, 2020. Accessed January 20, 2024. https://www.fda.gov/news-events/press-announcements/fda-approves-first-pi3k-inhibitor-breast-cancer

148. Research C for DE and. duvelisib (COPIKTRA, Verastem, Inc.) for adult patients with relapsed or refractory chronic lymphocytic leukemia (CLL) or small lymphocytic lymphoma (SLL). *FDA*. Published online February 9, 2019. Accessed January 20, 2024. https://www.fda.gov/drugs/resources-

information-approved-drugs/duvelisib-copiktra-verastem-inc-adult-patients-relapsed-or-refractory-chronic-lymphocytic-leukemia

149. Yu M, Chen J, Xu Z, et al. Development and safety of PI3K inhibitors in cancer. *Arch Toxicol*. 2023;97(3):635-650. doi:10.1007/s00204-023-03440-4

150. Hemmings BA, Restuccia DF. PI3K-PKB/Akt Pathway. *Cold Spring Harb Perspect Biol*. 2012;4(9):a011189. doi:10.1101/cshperspect.a011189

151. Gregory MA, Qi Y, Hann SR. Phosphorylation by glycogen synthase kinase-3 controls c-myc proteolysis and subnuclear localization. *J Biol Chem*. 2003;278(51):51606-51612. doi:10.1074/jbc.M310722200

152. Peng Y, Wang Y, Zhou C, Mei W, Zeng C. PI3K/Akt/mTOR Pathway and Its Role in Cancer Therapeutics: Are We Making Headway? *Front Oncol*. 2022;12:819128. doi:10.3389/fonc.2022.819128

153. Ruvinsky I, Meyuhas O. Ribosomal protein S6 phosphorylation: from protein synthesis to cell size. *Trends in Biochemical Sciences*. 2006;31(6):342-348. doi:10.1016/j.tibs.2006.04.003

154. Zhou H, Huang S. The complexes of mammalian target of rapamycin. *Curr Protein Pept Sci*. 2010;11(6):409-424. doi:10.2174/138920310791824093

155. Cross DA, Alessi DR, Cohen P, Andjelkovich M, Hemmings BA. Inhibition of glycogen synthase kinase-3 by insulin mediated by protein kinase B. *Nature*. 1995;378(6559):785-789. doi:10.1038/378785a0

156. Roussel MF, Davis JN, Cleveland JL, Ghysdael J, Hiebert SW. Dual control of myc expression through a single DNA binding site targeted by ets family proteins and E2F-1. *Oncogene*. 1994;9(2):405-415.

157. Krumm A, Meulia T, Brunvand M, Groudine M. The block to transcriptional elongation within the human c-myc gene is determined in the promoter-proximal region. *Genes Dev*. 1992;6(11):2201-2213. doi:10.1101/gad.6.11.2201

158. Albert T, Mautner J, Funk JO, Hörtnagel K, Pullner A, Eick D. Nucleosomal structures of c-myc promoters with transcriptionally engaged RNA polymerase II. *Mol Cell Biol*. 1997;17(8):4363-4371. doi:10.1128/MCB.17.8.4363

159. Strobl LJ, Eick D. Hold back of RNA polymerase II at the transcription start site mediates down-regulation of c-myc in vivo. *EMBO J*. 1992;11(9):3307-3314. doi:10.1002/j.1460-2075.1992.tb05409.x

160. Cutry AF, Kinniburgh AJ, Krabak MJ, Hui SW, Wenner CE. Induction of c-fos and c-myc proto-oncogene expression by epidermal growth factor and transforming growth factor alpha is calcium-independent. *J Biol Chem*. 1989;264(33):19700-19705.

161. Eick D, Berger R, Polack A, Bornkamm GW. Transcription of c-myc in human mononuclear cells is regulated by an elongation block. *Oncogene*. 1987;2(1):61-65.

162. Heckford SE, Gelmann EP, Matis LA. Distinct mechanisms of c-myc and lymphokine gene expression in an antigen specific T cell clone. *Oncogene*. 1988;3(4):415-421.

163. Spencer CA, Groudine M. Control of c-myc Regulation in Normal and Neoplastic Cells. In: Vande Woude GF, Klein G, eds. *Advances in Cancer Research*. Vol 56. Academic Press; 1991:1-48. doi:10.1016/S0065-230X(08)60476-5

164. Albert T, Wells J, Funk JO, et al. The Chromatin Structure of the Dual c-myc Promoter P1/P2 Is Regulated by Separate Elements*. *Journal of Biological Chemistry*. 2001;276(23):20482-20490. doi:10.1074/jbc.M100265200

165. Wright CJM, McCormack PL. Trametinib: first global approval. *Drugs*. 2013;73(11):1245-1254. doi:10.1007/s40265-013-0096-1

166. Definition of trametinib dimethyl sulfoxide - NCI Drug Dictionary - NCI. Published February 2, 2011. Accessed January 16, 2024. https://www.cancer.gov/publications/dictionaries/cancer-drug/def/trametinib-dimethyl-sulfoxide

167. Advani VM, Ivanov P. Translational control under stress: reshaping the translatome. *Bioessays*. 2019;41(5):e1900009. doi:10.1002/bies.201900009

168. Kazemi S, Mounir Z, Baltzis D, et al. A Novel Function of eIF2α Kinases as Inducers of the Phosphoinositide-3 Kinase Signaling Pathway. *Mol Biol Cell*. 2007;18(9):3635-3644. doi:10.1091/mbc.E07-01-0053

169. Iacono M, Mignone F, Pesole G. uAUG and uORFs in human and rodent 5′untranslated mRNAs. *Gene*. 2005;349:97-105. doi:10.1016/j.gene.2004.11.041

170. Graczyk D, Cieśla M, Boguta M. Regulation of tRNA synthesis by the general transcription factors of RNA polymerase III - TFIIIB and TFIIIC, and by the MAF1 protein. *Biochim Biophys Acta Gene Regul Mech*. 2018;1861(4):320-329. doi:10.1016/j.bbagrm.2018.01.011

171. Orioli A. tRNA biology in the omics era: Stress signalling dynamics and cancer progression. *Bioessays*. 2017;39(3). doi:10.1002/bies.201600158

172. Torrent M, Chalancon G, de Groot NS, Wuster A, Babu MM. Cells alter their tRNA abundance to selectively regulate protein synthesis during stress conditions. *Sci Signal*. 2018;11(546):eaat6409. doi:10.1126/scisignal.aat6409

173. Ruusala T, Andersson D, Ehrenberg M, Kurland CG. Hyper-accurate ribosomes inhibit growth. *EMBO J*. 1984;3(11):2575-2580.

174. Wohlgemuth I, Pohl C, Mittelstaet J, Konevega AL, Rodnina MV. Evolutionary optimization of speed and accuracy of decoding on the ribosome. *Philos Trans R Soc Lond B Biol Sci*. 2011;366(1580):2979-2986. doi:10.1098/rstb.2011.0138

175. Lee YS, Shibata Y, Malhotra A, Dutta A. A novel class of small RNAs: tRNA-derived RNA fragments (tRFs). *Genes Dev*. 2009;23(22):2639-2649. doi:10.1101/gad.1837609

176. Sun C, Fu Z, Wang S, et al. Roles of tRNA-derived fragments in human cancers. *Cancer Lett*. 2018;414:16-25. doi:10.1016/j.canlet.2017.10.031

177. OZANICK S, KRECIC A, ANDERSLAND J, ANDERSON JT. The bipartite structure of the tRNA m1A58 methyltransferase from S. cerevisiae is conserved in humans. *RNA*. 2005;11(8):1281-1290. doi:10.1261/rna.5040605

178. Types of Non-Hodgkin Lymphoma in Children and Teens. Accessed January 30, 2024. https://www.cancer.org/cancer/types/childhood-non-hodgkin-lymphoma/about/types-non-hodgkin-children.html

179. Kim H, Park ES, Lee SH, et al. Clinical Outcome of Relapsed or Refractory Burkitt Lymphoma and Mature B-Cell Lymphoblastic Leukemia in Children and Adolescents. *Cancer Res Treat*. 2014;46(4):358-365. doi:10.4143/crt.2013.047

180. Möker P, zur Stadt U, Zimmermann M, et al. Characterization of IG-MYC-breakpoints and their application for quantitative minimal disease monitoring in high-risk pediatric Burkitt-lymphoma and. *Leukemia*. 2022;36(9):2343-2346. doi:10.1038/s41375-022-01626-w

181. Frys S, Czuczman NM, Mavis C, et al. Deregulation of the PI3K/Akt Signal Transduction Pathway Is Associated with the Development of

Chemotherapy Resistance and Can be Effectively Targeted to Improve Chemoresponsiveness in Burkitt Lymphoma Pre-Clinical Models. *Blood*. 2014;124(21):1769. doi:10.1182/blood.V124.21.1769.1769

182. Bhatti M, Ippolito T, Mavis C, et al. Pre-clinical activity of targeting the PI3K/Akt/mTOR pathway in Burkitt lymphoma. *Oncotarget*. 2018;9(31):21820-21830. doi:10.18632/oncotarget.25072

183. Qiao Q, Jiang Y, Li G. Inhibition of the PI3K/AKT-NF-κB pathway with curcumin enhanced radiation-induced apoptosis in human Burkitt's lymphoma. *J Pharmacol Sci*. 2013;121(4):247-256. doi:10.1254/jphs.12149fp